

1
2
3
4
5
6
7
8
9
10
11
12
13
14
15
16
17
18
19
20
21
22
23
24
25
26
27
28
29

Cover Page

Title: Long-Distance Electrical and Calcium Signals Evoked by Hydrogen Peroxide in Physcomitrella

Short title: Hydrogen peroxide-evoked signals in Physcomitrella

Corresponding author: M. Koselski

Department of Plant Physiology and Biophysics, Institute of Biological Sciences, Maria Curie-Skłodowska University, Akademicka 19, Lublin/20-033, Poland, Telephone: (+48)815375955, Email address: mateusz.koselski@poczta.umcs.lublin.pl

Subject areas: cell–cell interaction, membranes and transport

Number of black and white figures: 3

Number of colour figures: 3

Number of tables: 3

Number of supplementary materials: 5 figures, 7 videos, 1 table

30
31
32
33
34
35
36
37
38
39
40
41
42
43
44
45
46
47
48
49
50
51
52
53
54
55
56
57
58
59

Title Page

Title: Long-Distance Electrical and Calcium Signals Evoked by Hydrogen Peroxide in Physcomitrella

Short title: Hydrogen peroxide-evoked signals in Physcomitrella

Mateusz Koselski^{1*}, Sebastian N. W. Hoernstein², Piotr Wasko¹, Ralf Reski^{2,3}, Kazimierz Trębacz¹

1. Department of Plant Physiology and Biophysics, Institute of Biological Sciences, Maria Curie-Skłodowska University, Lublin, 20-033 Poland

2. Plant Biotechnology, Faculty of Biology, University of Freiburg, Schaezlestrasse 1, 79104, Freiburg, Germany

3. Signalling Research Centres BIOSS and CIBSS, Schaezlestrasse 18, 79104, Freiburg, Germany

Corresponding author: Mateusz Koselski

Email address: mateusz.koselski@poczta.umcs.lublin.pl

ORCID-IDs:

Mateusz Koselski: 0000-0002-7375-9136

Sebastian N. W. Hoernstein: 0000-0002-2095-689X

Piotr Wasko: 0009-0001-1605-9096

Ralf Reski: 0000-0002-5496-6711

Kazimierz Trębacz: 0000-0001-5642-9955

60 **Abstract**

61 Electrical and calcium signals in plants are one of the basic carriers of information transmitted
62 over a long distance. Together with reactive oxygen species (ROS) waves, electrical and
63 calcium signals can participate in cell-to-cell signaling, conveying information about different
64 stimuli, e.g. abiotic stress, pathogen infection, or mechanical injury. There is no information
65 on the ability of ROS to evoke systemic electrical or calcium signals in the model moss
66 *Physcomitrella* and on the relationships between these responses. Here, we show that external
67 application of hydrogen peroxide evokes electrical signals in the form of long-distance
68 changes in the membrane potential, which transmit through the plant instantly after
69 stimulation. The responses were calcium dependent, since their generation was inhibited by
70 lanthanum, a calcium channel inhibitor (2 mM) or EDTA, a calcium chelator (0.5 mM). The
71 electrical signals were partially dependent on glutamate receptor ion channels (GLR), since
72 the knockout of GLR genes only slightly reduced the amplitude of the responses. The basal
73 part of the gametophyte, which is rich in protonema cells, was the most sensitive to hydrogen
74 peroxide. The measurements carried out on the protonema expressing fluorescent calcium
75 biosensor GCaMP3 proved that. We also demonstrate upregulation of a stress-related gene
76 which appears in a distant section of the moss 8 minutes after H₂O₂ treatment. The results
77 help to understand the importance of both types of signals in the transmission of information
78 about the appearance of ROS in the plant cell apoplast.

79

80 **Keywords:** calcium imaging, cell-to-cell signaling, cell excitability, glutamate receptor,
81 hydrogen peroxide, stress-related genes

82

83 **Introduction**

84 As an early terrestrial plant, the moss *Physcomitrella* (new botanical name *Physcomitrium*
85 *patens*), from the beginning of the adaptation to land conditions, had to cope with exposure to
86 UV radiation, ozone, wounding, and many other abiotic and biotic stressors that enhance the
87 synthesis of reactive oxygen species (ROS) (Rensing et al., 2020, 2008; Tucker et al., 2005).
88 *Physcomitrella* is an emerging model plant with a fully sequenced genome (Rensing et al.,
89 2008; Lang et al., 2018). It is widely used to study defense mechanisms against environmental
90 stress factors (Frank et al., 2005; Hoernstein et al., 2023; Koselski et al., 2019; Saidi et al.,
91 2009). It was previously demonstrated in our lab that *Physcomitrella* is capable of generating
92 action potentials (APs) after illumination with light of sufficient (over-threshold) intensity,
93 cooling, glutamate (Glu) treatment, etc. (Koselski et al., 2020, 2019, 2008).
94 Electrophysiological experiments with the application of ion channel inhibitors and
95 manipulation of ion gradients across the plasma membrane indicated that Ca^{2+} fluxes from
96 external and internal stores were involved in the generation of APs in *Physcomitrella*. They
97 interacted with K^+ and, to a lesser extent, with Cl^- fluxes. Our recent study on GCaMP
98 mutants allowing monitoring of changes in the cytoplasmic Ca^{2+} concentration ($[\text{Ca}^{2+}]_{\text{cyt}}$)
99 demonstrated that local Glu application caused an increase in $[\text{Ca}^{2+}]_{\text{cyt}}$ confined to the site of
100 the Glu treatment, whereas AP was transmitted to distant cells (Koselski et al., 2020). This
101 was rather an unexpected result, because in other plant species examined before, action
102 potentials or variation potentials (VPs, known also as Slow Wave Potentials, SWPs) spread
103 together with Ca^{2+} waves and seem mutually dependent (Choi et al., 2017, 2014; Gilroy et al.,
104 2016). In the model vascular plant *Arabidopsis thaliana* two glutamate receptors *AtGLR3.3*
105 and *AtGLR3.6* were identified as key players in wound-induced SWP generation and
106 transmission (Farmer et al., 2020; Mousavi et al., 2013). Both genes are predominantly
107 expressed in vascular tissues: phloem and xylem contact cells, respectively. Glutamate (and
108 other amino acids) released from wounded tissues binds to the Ligand Binding Domain
109 (LBD) subunit of the glutamate receptor-like channels facilitating opening of the channel pore
110 and in consequence initiating a Ca^{2+} wave and other downstream responses, like jasmonate
111 (JA) key genes and other stress-related gene expressions (Grenzi et al., 2022).

112 According to the recent findings, in vascular plants, in addition to the ion fluxes facilitating
113 regenerative $[\text{Ca}^{2+}]_{\text{cyt}}$ wave formation and transmission, the ROS based component
114 supplements the long-distance signaling system (Baxter et al., 2014; Gilroy et al., 2016;
115 Kurusu et al., 2015; Marcec et al., 2019). NADPH oxidases (respiratory burst oxidase

116 homologs, RBOHs) localized in the plasma membrane seem to be good candidates to fit this
117 scheme. RBOHs cause reduction of oxygen to superoxide anion (O_2^-), which is quickly
118 converted to H_2O_2 . They possess EF-hand motives which activate them upon binding of Ca^{2+}
119 to enhance ROS production (Marcec et al., 2019; Wojtaszek, 1997). Before the machinery of
120 ROS scavenging reduces the ROS level back to normal, its temporary excess affects many
121 metabolic and signaling pathways and their components. H_2O_2 produced in the apoplast can
122 be quickly transported to the cytosol via aquaporins (Tian et al., 2016). Recently, a specific
123 apoplastic H_2O_2 receptor was discovered, Hydrogen-Peroxide-Induced Ca^{2+} Increases 1
124 (HPCA1) (Wu et al. 2020). It is a membrane-spanning protein composed of an extracellular
125 H_2O_2 sensor and a cytoplasmic kinase component, which is postulated to activate Ca^{2+} -
126 permeable channels after H_2O_2 binding to the sensor (Foyer, 2020; Wu et al., 2020). Thus, ion
127 channels can be affected from both sides of the plasma membrane. It was previously
128 demonstrated that ROS can activate ion channels in different plant species classified in
129 different branches of the phylogenetic tree of characean algae (Demidchik et al., 1997) to
130 dicots and monocots (Wu et al., 2015).

131 In vascular plants, hydrogen peroxide and hydroxyl radicals affect Ca^{2+} -permeable channels
132 in the plasma membrane and in the internal store – the vacuole. In *Arabidopsis thaliana*, two
133 classes of non-selective calcium-permeable channels are postulated to be involved: GLR
134 channels activated by glutamate and cyclic nucleotide-gated channels CNGCs (Finka et al.,
135 2012; Mousavi et al., 2013). Additionally, annexin1 has been reported to be involved in ROS-
136 induced $[Ca^{2+}]_{cyt}$ elevation (Richards et al., 2014). It has been demonstrated that homologs of
137 GLU and CNGC channels were involved in signaling processes in *Physcomitrella* (Finka and
138 Goloubinoff, 2014; Koselski et al., 2020; Ortiz-Ramírez et al., 2017). In addition to calcium-
139 permeable channels, K^+ channels in the plasma membrane have been found to respond to an
140 increase in the ROS level (Demidchik et al., 2010). Massive K^+ efflux in ROS-treated plants
141 was one of the first observations of plant response to this type of stress factors (Demidchik et
142 al., 2010; Nassery, 1979). In *Arabidopsis*, GORK (Guard Cell Outward Rectifying K^+) and
143 SKOR (Stellar Potassium Outward Rectifier) channels have been identified to be responsible
144 for that effect (Demidchik, 2018). These channels are also regarded as good candidates to
145 pass an outward current during the AP repolarization phase in excitable plants (Cuin et al.,
146 2018).

147 In the present study, we examined the effects of H_2O_2 treatment of intact *Physcomitrella*.
148 Electrical potential changes and $[Ca^{2+}]_{cyt}$ transients were measured in wild type plants (WT)

149 and *glrI^{KO}* mutants treated with H₂O₂. We demonstrated that in the WT plants, H₂O₂ evoked
150 APs recorded both in the gametophyte leaves and protonema. The susceptibility of the
151 protonema to the treatment was much higher than in the leaf cells (0.5 mM versus 5 mM).
152 These signals were blocked by La³⁺ - a calcium channel inhibitor and by EDTA - a Ca²⁺
153 chelator. In the *glrI^{KO}* mutants, the electrical signals were reduced but not totally blocked,
154 which reveals that GLR channels are not crucial in H₂O₂-induced membrane potential
155 changes and Ca²⁺ fluxes in *Physcomitrella*. Involvement of other factors affecting [Ca²⁺]_{cyt} is
156 discussed. Looking for downstream effects of the signals, we demonstrate an enhanced
157 expression of stress-related genes.

158 **Results**

159 *Electrical signals in leaf cells*

160 The microelectrode measurements carried out on leaf (phylloid) cells from the *Physcomitrella*
161 gametophyte proved that the application of hydrogen peroxide evoked systemic electrical
162 signals in the form of membrane-potential changes transmitted along the plant. The long-
163 distance responses transmitted from the basal part of the plant (from the rhizoid side) and
164 recorded in apical leaf cells are presented in Fig. 1A. Experiments with different H₂O₂
165 concentrations indicate an influence of the concentration on amplitude and shape of
166 membrane potential changes recorded during the response. Stimulation of the basal part of the
167 plant with 0.05 mM and 0.1 mM H₂O₂ evoked irregular membrane potential changes with
168 similar amplitude, duration, and rate of depolarization (Fig. 1A, Tab 1). After an increase of
169 H₂O₂ concentration to 0.5 mM, significant changes in basic parameters describing the
170 membrane potential changes were obtained (Fig. 1A, Tab 1). The cell membrane depolarized
171 over twice as fast than in the lower concentrations (14.5±1.6 mV/s, n=18), and reached more
172 positive values. The amplitude of the depolarization amounted to 68±3 mV (n=19) and was
173 about 30 mV higher than after treatment with 0.05 and 0.1 mM, H₂O₂, respectively. Another
174 difference occurred in the shape of the responses, where after the peak of depolarization
175 evoked by 0.5 mM H₂O₂, a several-minute plateau of the membrane potential was recorded.
176 Hydrogen peroxide in the concentration of 0.5 mM was used to compare transmission ability
177 of electrical signals in the opposite direction - from the apical to the basal part of the plant
178 (Fig. 1B). The electrical signals transmitted from the apical part of the plant characterized in a
179 lower rate of depolarization (2.3±0.4 mV/s, n=8), amplitude (22±5 mV, n=9) and more
180 negative values of maximum depolarization (-142±8 mV, n=9). The additional feature was an

181 absence of a characteristic plateau of the membrane potential. The shape of the membrane
182 potential changes resembled the responses obtained after direct stimulation of a cell in the
183 apical part of the plant (Fig. 1C) or removing of the basal part (Fig. 1D), where a 10-fold
184 increase in the H₂O₂ concentration (to 5 mM) evoked responses similar to these transmitted
185 from the basal part after 0.5 mM H₂O₂ administration. These results indicate that the highest
186 susceptibility to hydrogen peroxide occurs in the basal part of the plant having protonema
187 cells and rhizoids, which act as an initial place for the generation of long-distance electrical
188 signals propagated toward the plant apex. The results also showed that an increase of the
189 H₂O₂ concentration facilitates generation of fully developed responses resembling action
190 potentials (APs).

191 Action potentials belong to the basic long-distance electrical signals recorded in plant cells
192 whose generation is dependent on an influx of calcium ions into the cytoplasm. We decided to
193 study the dependence of the recorded responses on the presence of an inhibitor of calcium
194 channels (2 mM lanthanum) or a calcium chelator (0.5 mM EDTA), respectively (Fig. 2 A,
195 B). Apart from effects of lanthanum and EDTA, the possibility to reverse the evoked effects
196 was also examined. Each plant was stimulated twice - after initial immersion for 3-4 hours in
197 lanthanum or EDTA, and then after the exchange of the solution back to the standard solution.
198 Immersion of the plants in lanthanum caused a total blockage of the response in 10 of the 19
199 tested cells. The responses in the other plants had a significantly reduced amplitude (to 9 ± 2
200 mV, n=9). Lanthanum also shifted the resting potential to positive values (to $-130 \pm 3 \pm$ mV,
201 n=19). The depolarization after the lanthanum application was slower (the rate amounted to
202 $0.5 \pm 0.2 \pm$ mV/s, n=8) and reached more negative values (-128 ± 5 , n=9). After a washout of
203 lanthanum from the measuring chamber, the amplitude of the responses increased to 27 ± 4 mV
204 (n=4), which indicated that inhibition of the responses by lanthanum is partially reversible.
205 EDTA totally blocked the responses in 9 of the 18 tested cells. Similar to lanthanum, EDTA
206 evoked reduction of the amplitude (to 13 ± 4 mV, n=9), shift of the resting potential to more
207 positive values (to $-122 \pm 5 \pm$ mV, n=18) and reduction of the rate of depolarization (to
208 $1.4 \pm 0.7 \pm$ mV/s, n=7). The shift of the resting potential after EDTA was partially reversible,
209 since a washout resulted in a restoration of the resting potential close to the values measured
210 in standard solution (-144 ± 4 mV, n=18). The comparison of all these parameters of the
211 membrane potential changes is compiled in Table 2.

212

213

214 *Electrical signals in protonema cells*

215 The results of the measurements carried out on the leaf cells indicated that it is hard to evoke
216 electrical signals in such cells, and the responses can start mainly from the protonema cells
217 and/or rhizoids - probably the target for the action of hydrogen peroxide. In order to study this
218 hypothesis, we decided to examine the effect of H₂O₂ on electrical membrane potential
219 changes in protonema cells. In these measurements, stimulation was carried out by
220 microinjection of H₂O₂ in three regions: initially into a chain of protonema cells adjacent to
221 the tested cell with the inserted microelectrode, then directly into the tested cell, and at the
222 end into the gametophyte base.

223 The results confirmed that, although electrical signals in the chain of protonema cells are
224 transmitted from cell to cell, the responses recorded in the same cell differed depending on the
225 region of stimulation (Fig. 4, Tab. 3, Supplementary Video S1). The stimulation of the
226 gametophyte base was the most effective, as it evoked electrical signals in each tested cell
227 immediately upon stimulation. In comparison to the electrical signals recorded in the leaf
228 cells, the signals from the protonema reached a higher amplitude (81±4 mV, n=8) and
229 duration (486±100 s, n=8). Surprisingly, weaker effects were achieved by the direct
230 stimulation of the tested cell or the stimulation of adjacent cells located close to the tested
231 cell. This method of stimulation evoked electrical signals with a smaller amplitude (66±6 mV,
232 n=8) than when H₂O₂ was applied in the gametophyte base. The responses recorded in the
233 protonema after the direct or indirect stimulation also exhibited a low depolarization rate
234 (1.6±0.6 mV/s, n=8), which was lower than the responses to the stimulation of the basal part
235 of the gametophyte (9.3±2.5 mV/s, n=8) or than those recorded in the leaf cells. Cell-to-cell
236 transmission of the electrical signal evoked by stimulation of the single cells from the chain of
237 protonema cells was rarely recorded and occurred only in 2 out of 18 tested plants
238 (Supplementary Fig. 1 and Video 2).

239 One of the candidates responsible for cell-to-cell communication in plants is the GLR
240 receptor, which can act as a non-selective calcium-permeable channel. The participation of
241 the GLR receptor in the transmission of electrical signals recorded in our experiments was
242 tested with the use of a *glr1* mutant of *Physcomitrella* (*Pp_{glr1}^{KO}*). In the *Pp_{glr1}^{KO}* mutants, as
243 in the wild type (WT), electrical signals propagated from the base of the gametophyte to the
244 leaf and protonema cells (Fig. 3, 4, Supplementary Video S3). In comparison to WT,

245 electrical signals recorded in the leaf cells of *Ppglr1^{KO}* had a reduced amplitude (to 46 ± 3 mV,
246 $n=26$) and a lower depolarization rate (9.6 ± 1.2 mV/s, $n=24$). The amplitude and rate of
247 depolarization of responses in the protonema cells from *Ppglr1^{KO}* recorded after the
248 stimulation of the basal gametophyte part reached similar values to those recorded in the WT
249 protonema cells (78 ± 3 mV, $n=10$ and 8.9 ± 3 mV/s, $n=10$, respectively). As in the WT
250 protonema cells, the direct or indirect stimulation of the protonema cells from *Ppglr1^{KO}*
251 evoked a smaller amplitude (63 ± 4 mV, $n=10$) and a lower depolarization rate (1.1 ± 0.3 mV/s,
252 $n=10$) than after the stimulation of the basal part of the *Ppglr1^{KO}* gametophyte. All these
253 changes in the parameters of changes in membrane potential in the protonema cells are
254 presented in Table 3.

255 *Calcium signals*

256 Calcium signals were recorded in plants expressing GCaMP3, i.e. a fluorescent calcium
257 indicator. Fluorescence measurements of calcium signals recorded after the stimulation of the
258 basal part of the plant indicated that the application of 0.5 mM H₂O₂ evoked calcium waves
259 which propagated from cell to cell in thread-like protonema cells. In contrast to electrical
260 signals, the calcium signals were slower and appeared a few minutes after the application of
261 the stimulus (Fig. 5, Supplementary Video S4). In some plants, the calcium signals did not
262 start at the stimulation site but appeared at some distance from the stimulation, acting as a
263 new source for calcium waves. In such a situation, calcium wave propagation was observed in
264 both directions - into and from the stimulation site. The rate of calcium signals propagation
265 along the protonema towards the site of the stimulation was similar to that in the opposite
266 direction, reaching 5.5 ± 0.7 $\mu\text{m/s}$ ($n=4$) and 5.2 ± 0.3 $\mu\text{m/s}$ ($n=7$), respectively. A characteristic
267 trait of some recorded calcium signals was its decrement with distance (Supplementary Fig. 2,
268 Supplementary Video S5). As in the case of electrical signals, the observation of calcium
269 signals in the stimulated leaves was possible after the increase of the hydrogen peroxide
270 concentration to 5 mM (Supplementary Video S6). In turn, in contrast to electrical signals,
271 calcium signals in leaf cells after application of 0.5 mM H₂O₂ to the basal part of the plant
272 were observed occasionally only in several cells from single leaves, but never (in none of 30
273 tested plants) in all leaves (Supplementary Video S7).

274 *Expression of genes in distant regions of the moss*

275 To analyze whether the electrical signal which was triggered upon local treatment would be
276 accompanied by changes in gene expressions in distant tissues, we selected candidate genes

277 and performed quantitative real-time PCR (qPCR). The candidates were selected based on
278 homology to Arabidopsis genes differentially expressed after local stress stimulus (Zandalinas
279 et al., 2019). In that study, a high light stimulus was locally imposed on selected Arabidopsis
280 rosette leaves and changes in gene expression in the locally treated and the distant, non-
281 treated leaves (local and systemic response, respectively) were investigated by RNAseq
282 analysis. From this published list, we selected candidate genes which were upregulated in the
283 systemic response if their expression was also inducible via H₂O₂ treatment and depended on
284 the function of the respiratory burst oxidase homolog D (RBOHD). Here, the gene encoding a
285 galacturonosyltransferase-like 10 protein (AT3G28340) was 5-fold upregulated 5 minutes
286 after the light stress treatment (Zandalinas et al., 2019). In *Physcomitrella*, we identified four
287 homologous proteins (Pp3c5_28420V3.1, Pp3c25_14930V3.1, Pp3c16_25090V3.1,
288 Pp3c2_18670V3.1) via *BlastP* search (Altschul et al., 1997) against the *Physcomitrella*
289 proteome (Lang et al., 2018). In analogy to Zandalinas et al. (2019) we tested their
290 responsiveness to H₂O₂ treatment and submerged entire gametophores in 0.5 mM H₂O₂ for 8
291 minutes. Here, we employed hydroponic gametophore cultures and analyzed the expression of
292 the candidate genes with qPCR. Of the four *Physcomitrella* homologues, only one gene
293 (Supplementary Fig S3, Pp3c16_25090V3.1) exhibited a significant increase in gene
294 expression ($p = 0.0305$) and hence, was selected for further analysis. For Pp3c5_28420V3.1,
295 an increase in gene expression was detectable (Supplementary Fig S3) but the difference was
296 not significant. Nevertheless, this gene was included for further experiments.

297 For these two selected candidates we tested whether both genes are regulated in gametophore
298 sections distant from a local treatment with H₂O₂. Apices of gametophores were harvested
299 after treatment with 0.5 mM H₂O₂ at the base for 8 min (Supplementary Fig S4) as well as
300 corresponding untreated apices. A significant upregulation of Pp3c16_25090V3.1 ($p =$
301 0.00184) was observed (Fig. 6) whereas an upregulation of Pp3c5_28420V3.1 was indicated,
302 but was not statistically significant ($p = 0.06075$). Thus, a local stress stimulus (here: H₂O₂ at
303 the gametophore base) triggers alteration of gene expression within 8 minutes in distant
304 sections (here: apex) in *Physcomitrella*.

305 Discussion

306 Plant cell signaling is based mainly on generation and transmission of different types of
307 signals including electrical, calcium, and reactive oxygen species (ROS). Investigations of the
308 relationship between these signals allow unraveling signaling pathways triggered in response

309 to biotic and abiotic stresses. In this study, we tried to answer the question whether external
310 application of ROS (hydrogen peroxide) evokes systemic response in the form of electrical
311 and calcium signals, to analyze the interdependence of these signals and their impact on gene
312 expression in distant regions.

313 The importance of ROS in the plant defense system has been evidenced by many experiments
314 (Huang et al., 2019). One of the first studies focused on the involvement of ROS in cell-to-
315 cell communication in *Arabidopsis* (Miller et al., 2009) proved that local stimuli produced
316 ROS waves propagating through the plant at a rate of 8.4 cm/min and the response was
317 dependent on a gene RBOHD (Respiratory Burst Oxidase Homolog D) encoding plant
318 NADPH oxidase involved in the production of ROS. The rate of propagation of such
319 RBOHD-related ROS signals recorded in different tissues ranged from ~400 to 1400 $\mu\text{m}/\text{sec}$
320 and was dependent on the type of stress (Choi et al., 2017). Together with propagation of the
321 signal, the accumulation of extracellular ROS was observed along the path of the signal
322 (Miller et al., 2009), indicating that each cell along the path is able to activate RBOHD and
323 release ROS, which in turn trigger adjacent cells to carry out the same process. In such an
324 autopropagation process, named ROS-induced ROS-release (RIRR), hydrogen peroxide
325 generated by RBOHD can be regarded as a long-distance signal. However, in the study by
326 Miller et al. (2009), external application of H_2O_2 did not evoke a ROS wave indicating
327 involvement of some other signal molecules in the propagation of the ROS wave.

328 Calcium is a candidate for such a signal molecule and together with ROS can cooperate in
329 long-distance transmission of information about stimuli. For example, calcium-dependent
330 protein kinase CPK5 playing a role in plant immunity is important for cell-to-cell
331 communication based on ROS waves (Dubiella et al., 2013). There are also other ways of
332 activation of RBOH proteins by calcium, including direct binding of this ion to the EF-hand
333 motif on the RBOH protein (Kimura et al., 2012) or binding of phosphatidic acid to the same
334 protein whose accumulation in the cell can be induced by calcium (Zhang et al., 2009). In
335 addition to the calcium-induced ROS release process, ROS-induced calcium release is
336 possible. For example, it has been shown that ROS can activate different calcium permeable
337 channels, e.g. hyperpolarization-activated Ca^{2+} channels in root cells (Demidchik et al., 2007),
338 Ca^{2+} influx channels in guard cells (Pei et al., 2000), or Ca^{2+} permeable channels regulated by
339 annexin1 (Richards et al., 2014). Recent studies carried out on *Arabidopsis* allowed the
340 discovery of a plasma-membrane leucine-rich-repeat receptor kinase, i.e. hydrogen-peroxide
341 induced Ca^{2+} increase 1 (HPCA1), which links the perception of apoplasmic H_2O_2 with Ca^{2+}

342 signaling (Wu et al., 2020). One of the most probable mechanisms of the cooperation between
343 calcium and ROS in long-distance transmission of signals is that an increase in cytoplasmic
344 calcium evoked by a local stimulus can induce production of ROS via Ca^{2+} -RBOH
345 interactions and accumulation of ROS in the apoplast. The transport of ROS from the apoplast
346 to the cell, probably carried out by aquaporins or other channels, would evoke ROS-induced
347 calcium release, which in turn could induce ROS production (Gilroy et al., 2014).

348 As shown by the results of our study, H_2O_2 -evoked calcium signals are not systemic
349 responses, such as those observed earlier in *P. patens* under osmotic stress and salt
350 stimulation (Storti et al., 2018). Calcium waves with a velocity of about 400 $\mu\text{m/s}$ in response
351 to local salt stress were also measured in Arabidopsis (Choi et al., 2014), where blockage of
352 calcium channels by lanthanum inhibited not only the calcium waves but also the ROS-
353 regulated transcriptional marker (ZAT12), indicating that calcium and ROS waves are closely
354 linked. Assuming the interconnection of calcium signals and ROS waves, it is unlikely that
355 the extracellular application of H_2O_2 in our experiments evoked the ROS wave, since the
356 H_2O_2 -evoked calcium signals admittedly appeared at some distance from the stimulation site
357 but propagated with a decrement (Fig. 3). The other feature of the H_2O_2 -evoked calcium
358 signals in *Physcomitrella*, i.e. the slower rate of propagation than in the case of the ROS wave
359 (above 5 $\mu\text{m/s}$), also indicates a low probability of appearance of a calcium-associated ROS
360 wave. The ability to evoke local calcium signals but not self-propagating calcium waves by
361 the extracellular H_2O_2 application implies engagement of some other factors taking part in the
362 transmission of information about such stimuli. It seems that, in *P. patens*, electrical signals,
363 which appear at the moment of stimulation and propagate along the whole plant, are a proper
364 carrier of the information about H_2O_2 enhancement. There still remains the question of the
365 relationships between electrical, calcium, and ROS signals.

366 The relationship between ROS and electrical signals was previously confirmed in Arabidopsis
367 mutants lacking RBOHD, where propagating electrical signals after heat stress or high light
368 had a significantly reduced amplitude or were totally blocked in comparison to the wild type
369 (Suzuki et al., 2013). Taking into account the ability of extracellular ROS (mainly hydrogen
370 peroxide) to activate different ion channels (Demidchik, 2018), including calcium-permeable
371 channels which can participate in long-distance electrical signals, it seems that ROS can
372 promote electrical signals along the ROS wave path. This hypothesis can be also supported by
373 the similar velocity of different types of plant self-propagating electrical signals to the
374 velocity of the ROS wave [like action potentials (20-400 cm/min) and system potentials (5-10

375 cm/min); (Zimmermann et al., 2009)]. In *Physcomitrella*, the H₂O₂-evoked electrical signals
376 propagated immediately from the basal part along the whole plant (Fig. 1 and 2), indicating
377 that the signals appeared before the slowly propagating calcium waves. In cooperation with
378 ROS and calcium waves, electrical signals, which are probably the fastest carriers of
379 information, can initiate the whole array of plant defense responses. It is also probable that, by
380 reaching cells distant from the stimulation site, electrical signals initiate a calcium-wave
381 response only in some cells, in which the threshold of calcium signal generation is lower than
382 in other cells. The relevance of this assumption is proved by the features of some calcium
383 waves observed in the protonema cells, where at a distance from the stimulation site in the
384 basal part of the plant, only a few protonema cells in the thread-like chain generated calcium
385 signals propagating in two directions - into and out of the site of stimulation.

386 One of the candidates of ion channels participating in long-distance electrical signals in plants
387 are glutamate receptor-like channels (GLR), which was confirmed in experiments carried out
388 on *Arabidopsis* (Mousavi et al., 2013; Salvador-Recatalà, 2016; Salvador-Recatalà et al.,
389 2014). Wound-induced electrical signals recorded in this species were dependent on clade III
390 GLRs (GLR 3.3 and GLR 3.6) and played a crucial role in the distal production of jasmonates
391 taking part in plant defense responses (Mousavi et al., 2013). It is a matter of discussion if
392 those channels are directly responsible for Ca²⁺ fluxes since they are predominantly expressed
393 in endomembranes (Farmer et al., 2020; Nguyen et al., 2018).

394 In *Physcomitrella*, only two *GLR* genes have been identified (Verret et al., 2010). Both genes
395 (*PpGLR1* and *PpGLR2*) are paralogs to *GLR* clade III from *Arabidopsis* (De Bortoli et al.,
396 2016) and encode channels participating in chemotaxis and reproduction of *Physcomitrella*
397 (Ortiz-Ramírez et al., 2017). A patch-clamp study indicated that GLR1 is a calcium-
398 permeable ion channel localized in the cell membrane and partially inhibited by glutamate
399 receptor antagonists (Ortiz-Ramírez et al., 2017). These data indicate that GLR1 in
400 *Physcomitrella*, similar to GLR 3.3 and GLR 3.6 from *Arabidopsis*, can be important in the
401 transmission of long-distance electrical signals. This hypothesis was not fully confirmed in
402 our study, since H₂O₂ evoked long-distance electrical signals in the *Physcomitrella glr1^{KO}*
403 mutants; however, the response differed in the amplitude (Tab. 1). Such a "weak" effect of the
404 GLR1 receptor knockout suggests that, in addition to GLR channels, other channels must be
405 engaged in the long-distance propagation of ROS-induced electrical signals. The most
406 important channels taking part in the generation of electrical signals in *Physcomitrella* are
407 probably calcium-permeable, given the blockage of H₂O₂-evoked responses by the calcium

408 channel inhibitor (lanthanum) or the calcium chelator (EDTA) (Fig. 1D). It is also probable
409 that, in addition to ion channels in the plasma membrane, a significant role in the transmission
410 of electrical signals is assigned to intracellular calcium channels. One of the best-known
411 intracellular channels permeable e.g. to calcium is the two-pore channel 1 (TPC1) located in
412 the vacuolar membrane, the tonoplast (Dadacz-Narloch et al., 2011). A patch-clamp study
413 carried out in our laboratory demonstrated that TPC channels in *Physcomitrella* vacuoles
414 conduct Ca^{2+} currents (Koselski et al., 2013). Involvement of the channel in the transmission
415 of long-distance calcium waves has been demonstrated (Choi et al., 2014), but there is no
416 information about the role of TPC1 in the transmission of electrical signals. As calcium-
417 permeable channels, TPC1 may be involved in the release of calcium from intracellular
418 compartments (Qudeimat et al., 2008) leading to calcium-induced calcium release (CICR), a
419 desired phenomenon for long-distance signal transmission, but this assumption arouses
420 controversy (Pottosin et al., 1997; Ward et al., 1994). The role of H_2O_2 in CICR is
421 questionable since MIFE (Microelectrode Ion Flux Estimation) and patch-clamp studies
422 carried out on vacuoles from *Beta vulgaris* demonstrated that H_2O_2 suppressed the Ca^{2+} efflux
423 from the vacuole and slow vacuolar (SV) currents carried by TPC1 (Pottosin et al., 2009).

424 Effectively, the treatment with 0.5 mM H_2O_2 at the base of gametophores was sufficient to
425 trigger an increase in gene expression in the apex of a component of the homogalacturonan
426 biosynthesis (Fig. 6, Pp3c16_25090V3.1). Here, the homologous candidate
427 Pp3c5_28420V3.1 was not significantly upregulated although an increasing trend was
428 detectable. This agrees with publicly available data indicating that both genes are not co-
429 expressed. Galacturonosyltransferase-like proteins such as Pp3c16_25090V3.1 act in the
430 pectin assembly (homogalacturonan biosynthesis) of the primary cell wall (reviewed in Loix
431 et al., 2017). Under oxidative stress, cell-wall pectins also represent a source for the
432 biosynthesis of ascorbic acid (García-Caparrós et al., 2021; Valpuesta and Botella, 2004),
433 which in turn is used to detoxify ROS such as H_2O_2 . Both selected candidates are homologues
434 of an *Arabidopsis* isoform (AT3G28340) whose gene expression is regulated via ROS waves
435 (Zandalinas et al., 2019). However, it should be noted that Galacturonosyltransferase-like
436 proteins comprise a large gene family with at least 21 members in *Arabidopsis* and 17 genes
437 in *Physcomitrella* (Van Bel et al., 2022) and clear ortholog relations are not yet resolved. The
438 expression of the *Arabidopsis* homolog (AT3G28340) was 5-fold increased only in systemic
439 leaves distant from a local high light stress impulse (Zandalinas et al., 2019) and those data
440 further indicate that the increase of expression was a response to a ROS wave. In contrast, the

441 two selected homologues in *Physcomitrella* were not regulated by high light stress
442 (Supplementary Fig S5) but their expression increased after heat stress. Heat stress in plants is
443 accompanied by the elevated production of reactive oxygen species (ROS) such as H₂O₂
444 (reviewed in Mittler et al., 2022). In summary, these data show that the gene expression of at
445 least one of the two *Physcomitrella* candidates (Pp3c16_25090V3.1) is responsive to ROS.
446 Consequently, the increase of expression in the untreated apex (Fig. 6) was likely based on a
447 propagating ROS-wave.

448 Taken together, our study demonstrates differences in the generation and propagation of
449 H₂O₂-evoked electrical and calcium signals in the model moss *Physcomitrella*. Many of the
450 applied variants of measurements indicated that the basal part of the gametophyte is the most
451 excitable region, probably because a large number of protonema cells are juvenile cells from
452 an early stage of new gametophyte development. In comparison to the leaf cells, the responses
453 in the protonema exhibited higher amplitudes and lasted longer, which may indicate higher
454 susceptibility of such cells to ROS (Table 2 and 3, Fig. 1 and 4). The main difference between
455 the electrical and calcium signals was the velocity of propagation, which was higher in the
456 electrical signals. The other difference was the ability to propagate without a decrement; in
457 contrast to the electrical signals, calcium signals diminished with distance, even if they
458 appeared in some distance from stimuli (Fig. 5, Supplementary Video S4 and S5). Given
459 these differences, we propose that H₂O₂-evoked long-distance electrical signals are the first to
460 reach distant regions of the plant and activate calcium signals, but not in every cell. The
461 protonema cells were the most susceptible to calcium signals, indicating that the signals play
462 a key role in young and developing cells. A similar observation was reported in our previous
463 work focused on glutamate-evoked calcium signals (Koselski et al., 2020). Electrical and
464 calcium signals were not the only effect of H₂O₂ application. Gene expression analysis proved
465 that apart from the signals, an increase of stress-related genes expression is observed in not
466 stimulated distant regions of plants (Fig. 6). The increase in the gene expression appeared
467 after 8 minutes - the time close to duration of electrical signals. Similar time scale of electrical
468 signals and genes expression, raises the question about interdependence of the both
469 phenomena.

470 **Materials and methods**

471 Cultivation of plant material used for electrophysiological and calcium imaging analysis

472 Physcomitrella gametophytes were grown on KNOP solid agar medium (Reski and Abel,
473 1985) in 160 mm diameter Petri dishes. The wild-type plants (WT) and knockout *glr1*
474 mutants (*Pp~~glr1~~^{KO}*) were used for the analysis of membrane potential changes in leaf and
475 protonema cells with use of the microelectrode technique. A Physcomitrella mutant
476 expressing GCaMP3 was used for the fluorescence imaging of changes in the calcium
477 concentration. The plants were grown in a growing chamber (Convion Adaptis A1000,
478 Convion, Winnipeg, Canada) at a photoperiod of 16/8 light/dark, with light intensity 50
479 $\mu\text{mol}/\text{m}^2 \text{ s}$, and at temperature set to 23°C.

480 Cultivation of plant material used for gene expression analysis

481 Physcomitrella WT protonema (new species name: *Physcomitrium patens* (Hedw.) Mitt.
482 (Medina et al., 2019); ecotype “Gransden 2004” was cultivated in Knop medium with
483 microelements. Knop medium (pH 5.8) containing 250 mg/L KH_2PO_4 , 250 mg/L KCl, 250
484 mg/L $\text{MgSO}_4 \times 7 \text{ H}_2\text{O}$, 1,000 mg/L $\text{Ca}(\text{NO}_3)_2 \times 4 \text{ H}_2\text{O}$ and 12.5 mg/L $\text{FeSO}_4 \times 7 \text{ H}_2\text{O}$ was
485 prepared as described (Reski and Abel, 1985) and 10 mL per litre of a microelement (ME)
486 stock solution (309 mg/L H_3BO_3 , 845 mg/L $\text{MnSO}_4 \times 1 \text{ H}_2\text{O}$, 431 mg/L $\text{ZnSO}_4 \times 7 \text{ H}_2\text{O}$, 41.5
487 mg/L KI, 12.1 mg/L $\text{Na}_2\text{MoO}_4 \times 2 \text{ H}_2\text{O}$, 1.25 mg/L $\text{CoSO}_4 \times 5 \text{ H}_2\text{O}$, 1.46 mg/L $\text{Co}(\text{NO}_3)_2 \times 6$
488 H_2O) as described (Egener et al., 2002; Schween et al., 2003). The suspension culture was
489 dispersed weekly with an ULTRA-TURRAX (IKA) at 18,000 rpm for 90 s.

490 Hydroponic cultures of Physcomitrella gametophores were cultivated as described in
491 Hoernstein et al. (2023). Glass rings covered with mesh (PP, 250 m mesh, 215 m thread, Zitt
492 Thoma GmbH, Freiburg, Germany) were prepared as described in Erxleben et al. (2012).
493 Protonema suspension was adjusted to a final density of 440 mg/L (dry weight per volume) as
494 described (Decker et al., 2017) and evenly distributed in equal volumes on the mesh surface.
495 Glass rings covered with protonema were placed in Magenta[®] Vessels (Sigma-Aldrich, St.
496 Louis, USA). KnopME medium was supplemented until it touched the bottom of the mesh.
497 The medium was changed every 4 weeks.

498 Suspension cultures and hydroponic cultures were cultivated under standard light conditions
499 ($55 \mu\text{mol photons}/\text{m}^2 \text{ s}$) at 22°C in a 16h/8h light/dark cycle.

500 Measurements of membrane potential in leaf cells

501 The method of membrane-potential measurements with microelectrodes was similar to that
502 employed in Koselski et al. (2020). Plastic Petri dishes used in the microelectrode

503 measurements were divided into two chambers with a barrier. The barrier had a small (1 mm
504 width) gap sealed with Vaseline. Before the experiments the plants were incubated for 3-6
505 hours at light intensity of $50 \mu\text{mol}/\text{m}^2$ in a bath solution containing (in mM) 1 KCl, 1 CaCl₂,
506 50 sorbitol, and 2 HEPES, pH 7.5 (buffered by Tris). The stimuli were introduced by
507 application of 500 μL of a bath solution supplemented with 0.5 mM hydrogen peroxide. The
508 lanthanum chloride or EDTA influence on the H₂O₂-evoked responses described in this study
509 was assessed by application of one of these substances into one of the Petri dish
510 compartments containing the basal part of the plant. Borosilicate glass capillaries (1B150F-6,
511 World Precision Instruments, Sarasota, USA) were used to make micropipettes with the use
512 of a P-30 micropipette puller (Shutter Instrument Co., Novato, USA), filled with 100 mM
513 KCl, and connected to the FD223 electrometer (World Precision Instruments, Sarasota, USA).
514 A Sensapex SMX (Sensapex, Oulu, Finland) electronic micromanipulator was used for
515 positioning and insertion of the microelectrode. The reference electrode was composed of an
516 Ag/AgCl₂ wire inside a plastic tube filled with 100 mM KCl and ending with a porous tip.
517 The measured data were acquired by a Lab-Trax-4 device (World Precision Instruments,
518 Sarasota, USA) working with LabScribe2 software, which also allowed analyses of the data.
519 The analysis of statistical differences was performed in SigmaStat 4.0 (Systat Software Inc.,
520 California, USA). Recordings of changes in the membrane potential were recorded with 2 Hz
521 data collection frequency. Figures were prepared with the use of Sigma Plot 9.0 (Systat
522 Software Inc., California, USA) and CorelDraw12 (Corel Corporation, Ottawa, Canada)
523 software.

524 Measurements of membrane changes in protonema cells

525 The plants were prepared in the same way as for the measurements carried out on the leaves.
526 The microelectrode was positioned and inserted using a PatchStar (Scientifica, East Sussex,
527 UK) micromanipulator and observed under an Olympus IX71 (Tokyo, Japan) microscope
528 with a camera (Artcam-500MI, Tokyo, Japan) working with QuickPhoto Camera software
529 (version 2.3, Promicra, Prague, Czech Republic). A CellTram Vario microinjector
530 (Eppendorf, Hamburg, Germany) with a borosilicate glass micropipette (with a diameter of
531 about 3 μm) was used for the application of H₂O₂ onto the cell surface. Likewise, in our
532 previous paper (Koselski et al. 2020), 1 mM methyl blue was used for staining of the
533 stimulating solution, which allows observation of its dispersion. Live recording of membrane
534 potentials visible in LabScribe3 software and microscope camera images were recorded by
535 OBS software (ver. 23.2.1; Open Broadcaster Software, Massachusetts, USA).

536 Fluorescence calcium imaging

537 Films and images of calcium concentration changes in the GCaMP3 *P. patens* mutants were
538 recorded with the use of NIS-Elements AR software (ver.5.20.00 Nikon, Tokyo, Japan)
539 working with a Nikon Eclipse Ti fluorescence microscope equipped with a Nikon Plan UW
540 2X WD:7,5 objective and a Nikon DS-Ri2 camera (Nikon, Tokyo, Japan). The excitation of
541 fluorescence was provided by a Prior lumen 200 metal arc lamp (Prior Scientific Instruments
542 Ltd., Cambridge, England) and a 495-nm dichroic mirror with a standard GFP excitation filter
543 470 ± 20 nm. Images of fluorescence emission were recorded with 1-s exposure and a
544 standard GFP fluorescence emission barrier filter 525 ± 50 nm (Nikon, Tokyo, Japan).
545 Stimulation of the plants was carried out by microinjection using a CellTram Vario
546 microinjector (Eppendorf, Hamburg, Germany). The standard solution supplemented with
547 H_2O_2 was visible due to tinting by $0.025 \mu M$ fluorescein.

548 Treatment of plants used for gene expression analysis

549 Gametophores from hydroponic cultures were used for the treatment with H_2O_2 . Half of the
550 gametophores from one glass ring were cut approximately in the middle and only the upper
551 half of the gametophores (~ 100 mg) was used as control sample. Cut gametophore apices
552 were gently dried by dabbing with filter paper. The glass ring with the remaining uncut
553 gametophores was transferred into a new Magenta[®] Vessel containing KnopME with 0.5 mM
554 H_2O_2 . After eight minutes, the upper half of the remaining uncut gametophores (treated
555 sample) was harvested as described before. In total, gametophores from four independent
556 hydroponic cultures (four biological replicates) were sampled.

557 RNA extraction and quantitative real-time PCR (qPCR)

558 Extraction of RNA was done with the innuPREP Plant RNA Kit (Analytic Jena, Jena,
559 Germany) using the extraction buffer "PL". $5 \mu g$ total RNA were treated with DNaseI
560 (Thermo Fisher Scientific, Waltham, Massachusetts, U.S.) at $37^\circ C$ for 1 hour and integrity of
561 the RNA was checked on Agarose gels. $2 \mu g$ DNaseI digested RNA were used for reverse
562 transcription using the TaqMan[™] Reverse Transcription kit (N8080234, Thermo Fisher
563 Scientific) with random hexamer primers. Reverse transcription was performed at $42^\circ C$ for 1
564 hour. A non-transcribed control without the addition of MultiScribe[™]RT enzyme was
565 included. Primers for the qPCR were designed using Primer3Plus software
566 (<https://www.primer3plus.com/>, Untergasser et al., 2012) with qPCR settings and an

567 efficiency of 2 was confirmed using a 1:2 dilution series of cDNA. Melting curve analysis
568 was performed to exclude the presence of off-targets. qPCR was performed in 96-well plates
569 using the SensiFast™ SYBR No-ROX Kit (Bioline) in technical triplicates for each biological
570 replicate. 50 ng cDNA were used for each technical triplicate and the PCR reaction was
571 performed in a LightCycler® 480 (Roche, Basel, Switzerland). -RT and water controls for
572 each primer pair were included. The PCR reaction was performed in 45 cycles with a melting
573 temperature of 60°C. Expression analysis of the genes Pp3c5_28420V3 and
574 Pp3c16_25090V3 (genes of interest, GOI) was performed as described (Bohlender et al.,
575 2020) in relation to the housekeeping (reference) genes L21 (Pp3c13_2360V3, Beike et al.,
576 2015) and LWD (Pp3c22_18860V3, Schuessele et al., 2016). All primers are listed in
577 Supplementary Table 1. The expression levels were calculated relative to the reference genes
578 according to Livak and Schmittgen (2001) using the software for the LightCycler® 480
579 (V1.5.0, Roche). Relative expression is represented as $2^{(-\Delta CT)}$ with $\Delta CT = CT_{[GOI]} -$
580 $CT_{[reference]}$. Figure 6 was created and statistics were calculated in R (R Core Team, 2022).
581 Statistical significance was tested via one-way Anova with subsequent post-hoc test.
582 Significance was accepted at $p < 0.05$.

583 **Data Availability**

584 The data underlying this article are available in the article and in its online supplementary
585 material.

586 **Funding**

587 This work was supported by National Science Centre, Poland [grant DAINA 1 No.
588 2017/27/L/NZ1/03164] and by the German Research Foundation (DFG) under Germany's
589 Excellence Strategy (CIBSS – EXC-2189 – Project ID 390939984).

590 **Acknowledgments**

591 The authors thank Prof. José A. Feijó, Dr. Jörg D. Becker and Dr. Mário R. Santos for sharing
592 the glutamate receptor 1 (GLR1) knockout mutant of *Physcomitrella*. The authors thank Dr.
593 Thomas J. Kleist for providing the transgenic lines of *Physcomitrella* expressing GCaMP3.
594 We thank Richard Haas for performing the qPCR experiments and Anne Katrin Prowse for
595 language editing.

596 **Author contribution**

597 M.K. conceived and designed the manuscript, prepared the main part of experiments,
598 analyzed and interpreted the data, and drafted the main part of the work. P.W. participated in
599 preparation of the membrane potential measurements. K.T. participated in writing and revised
600 the manuscript. S. N. W. H and R. R. designed qPCR experiments, analyzed data and helped
601 writing the manuscript.

602 **Disclosures**

603 Conflicts of interest: No conflicts of interest declared

604

605 **References**

- 606 Altschul, S.F., Madden, T.L., Schäffer, A.A., Zhang, J., Zhang, Z., Miller, W., et al. (1997)
607 Gapped BLAST and PSI-BLAST: A new generation of protein database search
608 programs. *Nucleic Acids Res.* 25: 3389–3402.
- 609 Baxter, A., Mittler, R., and Suzuki, N. (2014) ROS as key players in plant stress signalling. *J*
610 *Exp Bot.* 65: 1229–1240.
- 611 Beike, A.K., Lang, D., Zimmer, A.D., Wüst, F., Trautmann, D., Wiedemann, G., et al. (2015)
612 Insights from the cold transcriptome of *Physcomitrella patens*: Global specialization
613 pattern of conserved transcriptional regulators and identification of orphan genes
614 involved in cold acclimation. *New Phytol.* 205: 869–881.
- 615 Van Bel, M., Silvestri, F., Weitz, E.M., Kreft, L., Botzki, A., Coppens, F., et al. (2022)
616 PLAZA 5.0: Extending the scope and power of comparative and functional genomics in
617 plants. *Nucleic Acids Res.* 50: D1468–D1474.
- 618 Bohlender, L.L., Parsons, J., Hoernstein, S.N.W., Rempfer, C., Ruiz-Molina, N., Lorenz, T.,
619 et al. (2020) Stable protein sialylation in *Physcomitrella*. *Front Plant Sci.* 11.
- 620 De Bortoli, S., Teardo, E., Szabò, I., Morosinotto, T., and Alboresi, A. (2016) Evolutionary
621 insight into the ionotropic glutamate receptor superfamily of photosynthetic organisms.
622 *Biophys Chem.* 218: 14–26.
- 623 Choi, W.G., Miller, G., Wallace, I., Harper, J., Mittler, R., and Gilroy, S. (2017) Orchestrating
624 rapid long-distance signaling in plants with Ca²⁺, ROS and electrical signals. *Plant J.* 90:
625 698–707.
- 626 Choi, W.G., Toyota, M., Kim, S.H., Hilleary, R., and Gilroy, S. (2014) Salt stress-induced
627 Ca²⁺ waves are associated with rapid, long-distance root-to-shoot signaling in plants.
628 *Proc Natl Acad Sci U S A.* 111: 6497–6502.
- 629 Cuin, T.A., Dreyer, I., and Michard, E. (2018) The role of potassium channels in *Arabidopsis*
630 *thaliana* long distance electrical signalling: AKT2 modulates tissue excitability while
631 GORK shapes action potentials. *Int J Mol Sci.* 19.
- 632 Dadacz-Narloch, B., Beyhl, D., Larisch, C., López-Sanjurjo, E.J., Reski, R., Kuchitsu, K., et
633 al. (2011) A novel calcium binding Site in the slow vacuolar cation channel TPC1 senses

- 634 luminal calcium levels. *Plant Cell*. 23: 2696–2707.
- 635 Decker, E.L., Alder, A., Hunn, S., Ferguson, J., Lehtonen, M.T., Scheler, B., et al. (2017)
636 Strigolactone biosynthesis is evolutionarily conserved, regulated by phosphate starvation
637 and contributes to resistance against phytopathogenic fungi in a moss, *Physcomitrella*
638 *patens*. *New Phytol.* 216: 455–468.
- 639 Demidchik, V. (2018) ROS-activated ion channels in plants: biophysical characteristics,
640 physiological functions and molecular nature. *Int J Mol Sci.* 19.
- 641 Demidchik, V., Cuin, T.A., Svistunenko, D., Smith, S.J., Miller, A.J., Shabala, S., et al.
642 (2010) Arabidopsis root K⁺-efflux conductance activated by hydroxyl radicals: Single-
643 channel properties, genetic basis and involvement in stress-induced cell death. *J Cell Sci.*
644 123: 1468–1479.
- 645 Demidchik, V., Shabala, S.N., and Davies, J.M. (2007) Spatial variation in H₂O₂ response of
646 *Arabidopsis thaliana* root epidermal Ca²⁺ flux and plasma membrane Ca²⁺ channels.
647 *Plant J.* 49: 377–386.
- 648 Demidchik, V., Sokolik, A., and Yurin, V. (1997) The Effect of Cu²⁺ on ion transport systems
649 of the plant cell plasmalemma. *Plant Physiol.* 114: 1313.
- 650 Dubiella, U., Seybold, H., Durian, G., Komander, E., Lassig, R., Witte, C.P., et al. (2013)
651 Calcium-dependent protein kinase/NADPH oxidase activation circuit is required for
652 rapid defense signal propagation. *Proc Natl Acad Sci U S A.* 110: 8744–8749.
- 653 Egner, T., Granado, J., Guitton, M.C., Hohe, A., Holtorf, H., Lucht, J.M., et al. (2002) High
654 frequency of phenotypic deviations in *Physcomitrella patens* plants transformed with a
655 gene-disruption library. *BMC Plant Biol.* 2: 1–9.
- 656 Erxleben, A., Gessler, A., Vervliet-Scheebaum, M., and Reski, R. (2012) Metabolite profiling
657 of the moss *Physcomitrella patens* reveals evolutionary conservation of osmoprotective
658 substances. *Plant Cell Rep.* 31: 427–436.
- 659 Farmer, E.E., Gao, Y.Q., Lenzoni, G., Wolfender, J.L., and Wu, Q. (2020) Wound- and
660 mechanostimulated electrical signals control hormone responses. *New Phytol.* 227:
661 1037–1050.
- 662 Finka, A., Cuendet, A.F.H., Maathuis, F.J.M., Saidi, Y., and Goloubinoff, P. (2012) Plasma

- 663 membrane cyclic nucleotide gated calcium channels control land plant thermal sensing
664 and acquired thermotolerance. *Plant Cell*. 24: 3333–3348.
- 665 Finka, A., and Goloubinoff, P. (2014) The CNGCb and CNGCd genes from *Physcomitrella*
666 *patens* moss encode for thermosensory calcium channels responding to fluidity changes
667 in the plasma membrane. *Cell Stress Chaperones*. 19: 83–90.
- 668 Foyer, C.H. (2020) Making sense of hydrogen peroxide signals. *Nature*. 578: 518–519.
- 669 Frank, W., Ratnadewi, D., and Reski, R. (2005) *Physcomitrella patens* is highly tolerant
670 against drought, salt and osmotic stress. *Planta*. 220: 384–394.
- 671 García-Caparrós, P., De Filippis, L., Gul, A., Hasanuzzaman, M., Ozturk, M., Altay, V., et al.
672 (2021) Oxidative stress and antioxidant metabolism under adverse environmental
673 conditions: a review. *Bot Rev*. 87: 421–466.
- 674 Gilroy, S., Białasek, M., Suzuki, N., Górecka, M., Devireddy, A.R., Karpiński, S., et al.
675 (2016) ROS, calcium, and electric signals: key mediators of rapid systemic signaling in
676 plants. *Plant Physiol*. 171: 1606–1615.
- 677 Gilroy, S., Suzuki, N., Miller, G., Choi, W.G., Toyota, M., Devireddy, A.R., et al. (2014) A
678 tidal wave of signals: calcium and ROS at the forefront of rapid systemic signaling.
679 *Trends Plant Sci*. 19: 623–630.
- 680 Grenzi, M., Bonza, M.C., and Costa, A. (2022) Signaling by plant glutamate receptor-like
681 channels: What else! *Curr Opin Plant Biol*. 68: 102253.
- 682 Hoernstein, S.N.W., Özdemir, B., van Gessel, N., Miniera, A.A., Rogalla von Bieberstein, B.,
683 Nilges, L., et al. (2023) A deeply conserved protease, acylamino acid-releasing enzyme
684 (AARE), acts in ageing in *Physcomitrella* and *Arabidopsis*. *Commun Biol*. 6: 61.
- 685 Huang, H., Ullah, F., Zhou, D.X., Yi, M., and Zhao, Y. (2019) Mechanisms of ROS
686 regulation of plant development and stress responses. *Front Plant Sci*. 10: 800.
- 687 Kimura, S., Kaya, H., Kawarazaki, T., Hiraoka, G., Senzaki, E., Michikawa, M., et al. (2012)
688 Protein phosphorylation is a prerequisite for the Ca²⁺-dependent activation of
689 *Arabidopsis* NADPH oxidases and may function as a trigger for the positive feedback
690 regulation of Ca²⁺ and reactive oxygen species. *Biochim Biophys Acta - Mol Cell Res*.
691 1823: 398–405.

- 692 Koselski, M., Trebacz, K., and Dziubinska, H. (2013) Cation-permeable vacuolar ion
693 channels in the moss *Physcomitrella patens*: a patch-clamp study. *Planta*. 238: 357–367.
- 694 Koselski, M., Trebacz, K., Dziubinska, H., and Krol, E. (2008) Light- and dark-induced
695 action potentials in *Physcomitrella patens*. *Plant Signal Behav.* 3: 13–18.
- 696 Koselski, M., Wasko, P., Derylo, K., Tchorzewski, M., and Trebacz, K. (2020) Glutamate-
697 induced electrical and calcium signals in the moss *Physcomitrella patens*. *Plant Cell*
698 *Physiol.* 61: 1807–1817.
- 699 Koselski, M., Wasko, P., Kupisz, K., and Trebacz, K. (2019) Cold- and menthol-evoked
700 membrane potential changes in the moss *Physcomitrella patens*: influence of ion channel
701 inhibitors and phytohormones. *Physiol Plant.* 167: 433–446.
- 702 Kurusu, T., Kuchitsu, K., and Tada, Y. (2015) Plant signaling networks involving Ca²⁺ and
703 Rboh/Nox-mediated ROS production under salinity stress. *Front Plant Sci.* 6.
- 704 Lang, D., Ullrich, K.K., Murat, F., Fuchs, J., Jenkins, J., Haas, F.B., et al. (2018) The
705 *Physcomitrella patens* chromosome-scale assembly reveals moss genome structure and
706 evolution. *Plant J.* 93: 515–533.
- 707 Livak, K.J., and Schmittgen, T.D. (2001) Analysis of relative gene expression data using real-
708 time quantitative PCR and the 2- $\Delta\Delta$ CT method. *Methods.* 25: 402–408.
- 709 Loix, C., Huybrechts, M., Vangronsveld, J., Gielen, M., Keunen, E., and Cuypers, A. (2017)
710 Reciprocal interactions between cadmium-induced cell wall responses and oxidative
711 stress in plants. *Front Plant Sci.* 8: 1–19.
- 712 Marcec, M.J., Gilroy, S., Poovaiah, B.W., and Tanaka, K. (2019) Mutual interplay of Ca²⁺
713 and ROS signaling in plant immune response. *Plant Sci.* 283: 343–354.
- 714 Medina, R., Johnson, M.G., Liu, Y., Wickett, N.J., Shaw, A.J., and Goffinet, B. (2019)
715 Phylogenomic delineation of Physcomitrium (Bryophyta: Funariaceae) based on targeted
716 sequencing of nuclear exons and their flanking regions rejects the retention of
717 *Physcomitrella*, *Physcomitridium* and *Aphanorrhagma*. *J Syst Evol.* 57: 404–417.
- 718 Miller, G., Schlauch, K., Tam, R., Cortes, D., Torres, M.A., Shulaev, V., et al. (2009) The
719 plant NADPH oxidase RBOHD mediates rapid systemic signaling in response to diverse
720 stimuli. *Sci Signal.* 2.

- 721 Mittler, R., Zandalinas, S.I., Fichman, Y., and Van Breusegem, F. (2022) Reactive oxygen
722 species signalling in plant stress responses. *Nat Rev Mol Cell Biol.* 23: 663–679.
- 723 Mousavi, S.A.R., Chauvin, A., Pascaud, F., Kellenberger, S., and Farmer, E.E. (2013)
724 GLUTAMATE RECEPTOR-LIKE genes mediate leaf-to-leaf wound signalling. *Nat*
725 *2013 5007463.* 500: 422–426.
- 726 Nassery, H. (1979) Salt-induced loss of potassium from plant roots. *New Phytol.* 83: 23–27.
- 727 Nguyen, C.T., Kurenda, A., Stolz, S., Chételat, A., and Farmer, E.E. (2018) Identification of
728 cell populations necessary for leaf-to-leaf electrical signaling in a wounded plant. *Proc*
729 *Natl Acad Sci U S A.* 115: 10178–10183.
- 730 Ortiz-Ramírez, C., Michard, E., Simon, A.A., Damineli, D.S.C., Hernández-Coronado, M.,
731 Becker, J.D., et al. (2017) GLUTAMATE RECEPTOR-LIKE channels are essential for
732 chemotaxis and reproduction in mosses. *Nat 2017 5497670.* 549: 91–95.
- 733 Pei, Z.M., Murata, Y., Benning, G., Thomine, S., Klüsener, B., Allen, G.J., et al. (2000)
734 Calcium channels activated by hydrogen peroxide mediate abscisic acid signalling in
735 guard cells. *Nature.* 406: 731–734.
- 736 Pottosin, I., Wherrett, T., and Shabala, S. (2009) SV channels dominate the vacuolar Ca²⁺
737 release during intracellular signaling. *FEBS Lett.* 583: 921–926.
- 738 Pottosin, I.I., Tikhonova, L.I., Hedrich, R., and Schönknecht, G. (1997) Slowly activating
739 vacuolar channels can not mediate Ca²⁺-induced Ca²⁺ release. *Plant J.* 12: 1387–1398.
- 740 Qudeimat, E., Faltusz, A.M.C., Wheeler, G., Lang, D., Brownlee, C., Reski, R., et al. (2008)
741 A PIBB-type Ca²⁺-ATPase is essential for stress adaptation in *Physcomitrella patens*.
742 *Proc Natl Acad Sci U S A.* 105: 19555–19560.
- 743 R Core Team. R: A language and environment for statistical computing (R Foundation for
744 Statistical Computing, 2022).
- 745 Rensing, S.A., Goffinet, B., Meyberg, R., Wu, S.Z., and Bezanilla, M. (2020) The moss
746 *Physcomitrium (Physcomitrella) patens*: a model organism for non-seed plants. *Plant*
747 *Cell.* 32: 1361–1376.
- 748 Rensing, S.A., Lang, D., Zimmer, A.D., Terry, A., Salamov, A., Shapiro, H., et al. (2008) The

- 749 Physcomitrella genome reveals evolutionary insights into the conquest of land by plants.
750 *Science*. 319: 64–69.
- 751 Reski, R. (1998) Development, genetics and molecular biology of mosses. *Bot Acta*. 111: 1–
752 15.
- 753 Reski, R., and Abel, W.O. (1985) Induction of budding on chloronemata and caulonemata of
754 the moss, *Physcomitrella patens*, using isopentenyladenine. *Planta 1985 1653*. 165: 354–
755 358.
- 756 Richards, S.L., Laohavisit, A., Mortimer, J.C., Shabala, L., Swarbreck, S.M., Shabala, S., et
757 al. (2014) Annexin 1 regulates the H₂O₂-induced calcium signature in *Arabidopsis*
758 *thaliana* roots. *Plant J*. 77: 136–145.
- 759 Saidi, Y., Finka, A., Muriset, M., Bromberg, Z., Weiss, Y.G., Maathuis, F.J.M., et al. (2009)
760 The heat shock response in moss plants is regulated by specific calcium-permeable
761 channels in the plasma membrane. *Plant Cell*. 21: 2829–2843.
- 762 Salvador-Recatalà, V. (2016) New roles for the GLUTAMATE RECEPTOR-LIKE 3.3, 3.5,
763 and 3.6 genes as on/off switches of wound-induced systemic electrical signals. *Plant*
764 *Signal Behav*. 11.
- 765 Salvador-Recatalà, V., Tjallingii, W.F., and Farmer, E.E. (2014) Real-time, in vivo
766 intracellular recordings of caterpillar-induced depolarization waves in sieve elements
767 using aphid electrodes. *New Phytol*. 203: 674–684.
- 768 Schuessele, C., Hoernstein, S.N.W., Mueller, S.J., Rodriguez-Franco, M., Lorenz, T., Lang,
769 D., et al. (2016) Spatio-temporal patterning of arginyl-tRNA protein transferase (ATE)
770 contributes to gametophytic development in a moss. *New Phytol*. 209: 1014–1027.
- 771 Schween, G., Hohe, A., Koprivova, A., and Reski, R. (2003) Effects of nutrients, cell density
772 and culture techniques on protoplast regeneration and early protonema development in a
773 moss, *Physcomitrella patens*. *J Plant Physiol*. 160: 209–212.
- 774 Storti, M., Costa, A., Golin, S., Zottini, M., Morosinotto, T., and Alboresi, A. (2018)
775 Systemic calcium wave propagation in *Physcomitrella patens*. *Plant Cell Physiol*. 59:
776 1377–1384.
- 777 Suzuki, N., Miller, G., Salazar, C., Mondal, H.A., Shulaev, E., Cortes, D.F., et al. (2013)

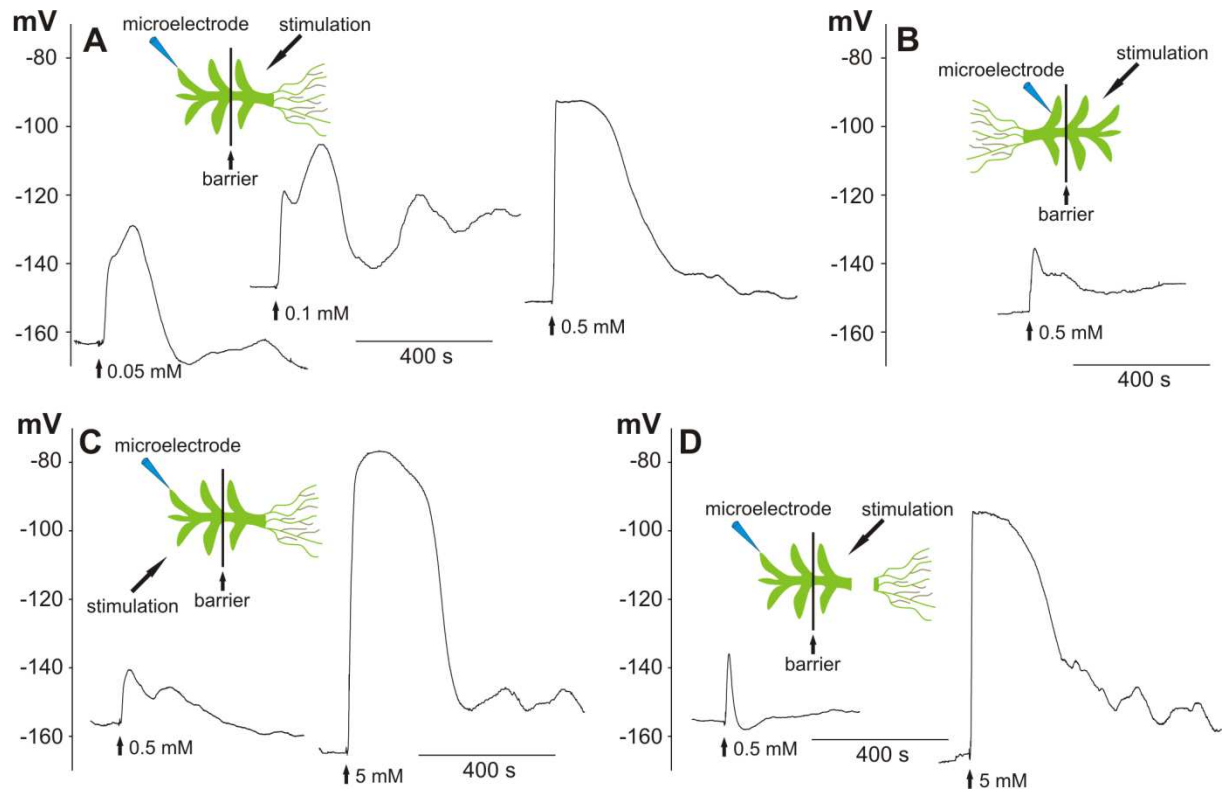
- 778 temporal-spatial interaction between reactive oxygen species and abscisic acid regulates
779 rapid systemic acclimation in plants. *Plant Cell*. 25: 3553–3569.
- 780 Tian, S., Wang, X., Li, P., Wang, H., Ji, H., Xie, J., et al. (2016) Plant aquaporin AtPIP1;4
781 links apoplastic H₂O₂ induction to disease immunity pathways. *Plant Physiol*. 171:
782 1635–1650.
- 783 Tucker, E.B., Lee, M., Alli, S., Sookhdeo, V., Wada, M., Imaizumi, T., et al. (2005) UV-A
784 induces two calcium waves in *Physcomitrella patens*. *Plant Cell Physiol*. 46: 1226–1236.
- 785 Untergasser, A., Cutcutache, I., Koressaar, T., Ye, J., Faircloth, B.C., Remm, M., et al. (2012)
786 Primer3-new capabilities and interfaces. *Nucleic Acids Res*. 40: 1–12.
- 787 Valpuesta, V., and Botella, M.A. (2004) Biosynthesis of L-ascorbic acid in plants: New
788 pathways for an old antioxidant. *Trends Plant Sci*. 9: 573–577.
- 789 Verret, F., Wheeler, G., Taylor, A.R., Farnham, G., and Brownlee, C. (2010) Calcium
790 channels in photosynthetic eukaryotes: implications for evolution of calcium-based
791 signalling. *New Phytol*. 187: 23–43.
- 792 Ward, J., Cell, J.S.-T.P., and 1994, undefined (1994) Calcium-activated K⁺ channels and
793 calcium-induced calcium release by slow vacuolar ion channels in guard cell vacuoles
794 implicated in the control of stomatal. *academic.oup.com*. 6: 669–683.
- 795 Wojtaszek, P. (1997) Mechanisms for the generation of reactive oxygen species in plant
796 defence response. *Acta Physiol Plant*. 4: 581–589.
- 797 Wu, F., Chi, Y., Jiang, Z., Xu, Y., Xie, L., Huang, F., et al. (2020) Hydrogen peroxide sensor
798 HPCA1 is an LRR receptor kinase in Arabidopsis. *Nature* 578: 577–581.
- 799 Wu, H., Shabala, L., Zhou, M., and Shabala, S. (2015) Chloroplast-generated ROS dominate
800 NaCl- induced K⁺ efflux in wheat leaf mesophyll. *Plant Signal Behav*. 10: 1–4.
- 801 Zandalinas, S.I., Sengupta, S., Burks, D., Azad, R.K., and Mittler, R. (2019) Identification
802 and characterization of a core set of ROS wave-associated transcripts involved in the
803 systemic acquired acclimation response of Arabidopsis to excess light. *Plant J*. 98: 126–
804 141.
- 805 Zhang, Y., Zhu, H., Zhang, Q., Li, M., Yan, M., Wang, R., et al. (2009) Phospholipase

806 dalphal and phosphatidic acid regulate NADPH oxidase activity and production of
807 reactive oxygen species in ABA-mediated stomatal closure in Arabidopsis. *Plant Cell*.
808 21: 2357–2377.

809 Zimmermann, M.R., Maischak, H., Mithöfer, A., Boland, W., and Felle, H.H. (2009) System
810 potentials, a novel electrical long-distance apoplastic signal in plants, induced by
811 wounding. *Plant Physiol.* 149: 1593.

812

813

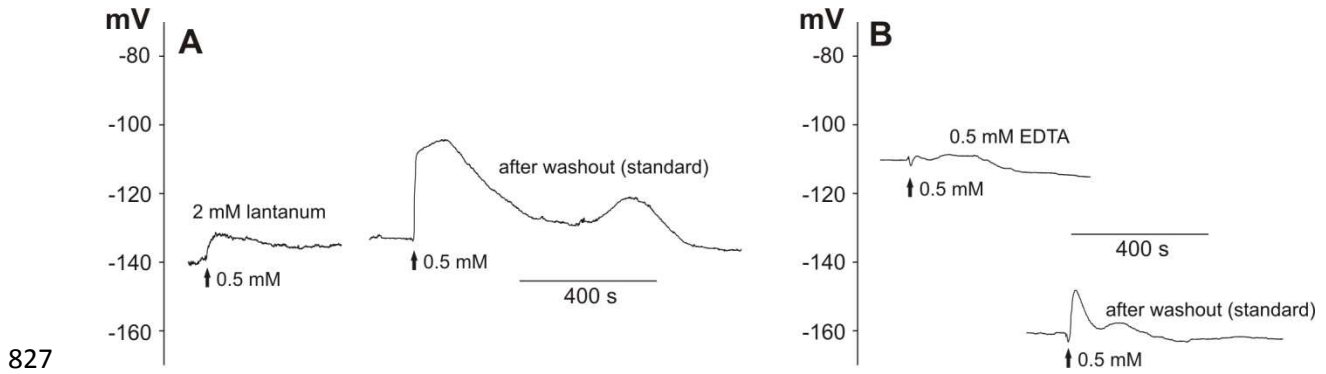


814

815 **Fig. 1.** Hydrogen peroxide-evoked long-distance electrical signals recorded in a
816 Physcomitrella leaf (phylloid) cell. The recordings were carried out in bipartite chambers with
817 a barrier separating two parts of the gametophyte. Schemes presenting the site of stimulation
818 and insertion of the microelectrode are in placed on the top of the recordings. A – long-
819 distance electrical signals in the form of membrane potential changes recorded after the
820 stimulation of the basal part of the gametophyte with different H₂O₂ concentrations. B -
821 electrical signals recorded after stimulation of the apical part of the gametophyte. C and D -
822 reduction of the sensitivity of the leaf cells to H₂O₂ recorded after direct stimulation of the
823 tested cell located in the apical part of the gametophyte and in the gametophyte with a cut-off
824 basal part, respectively. Vertical axes present the values of the membrane potential (in mV).

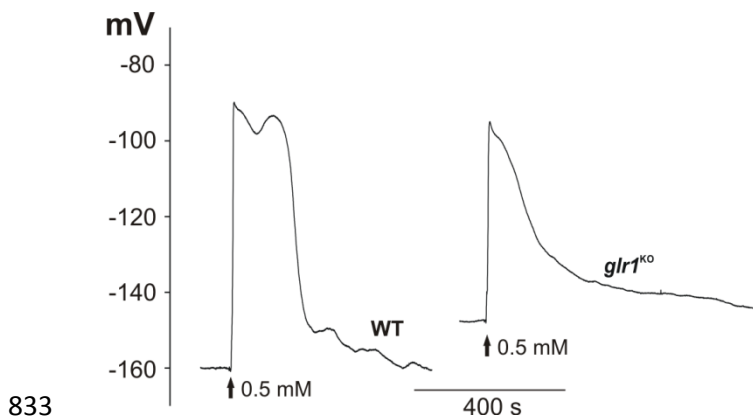
825

826

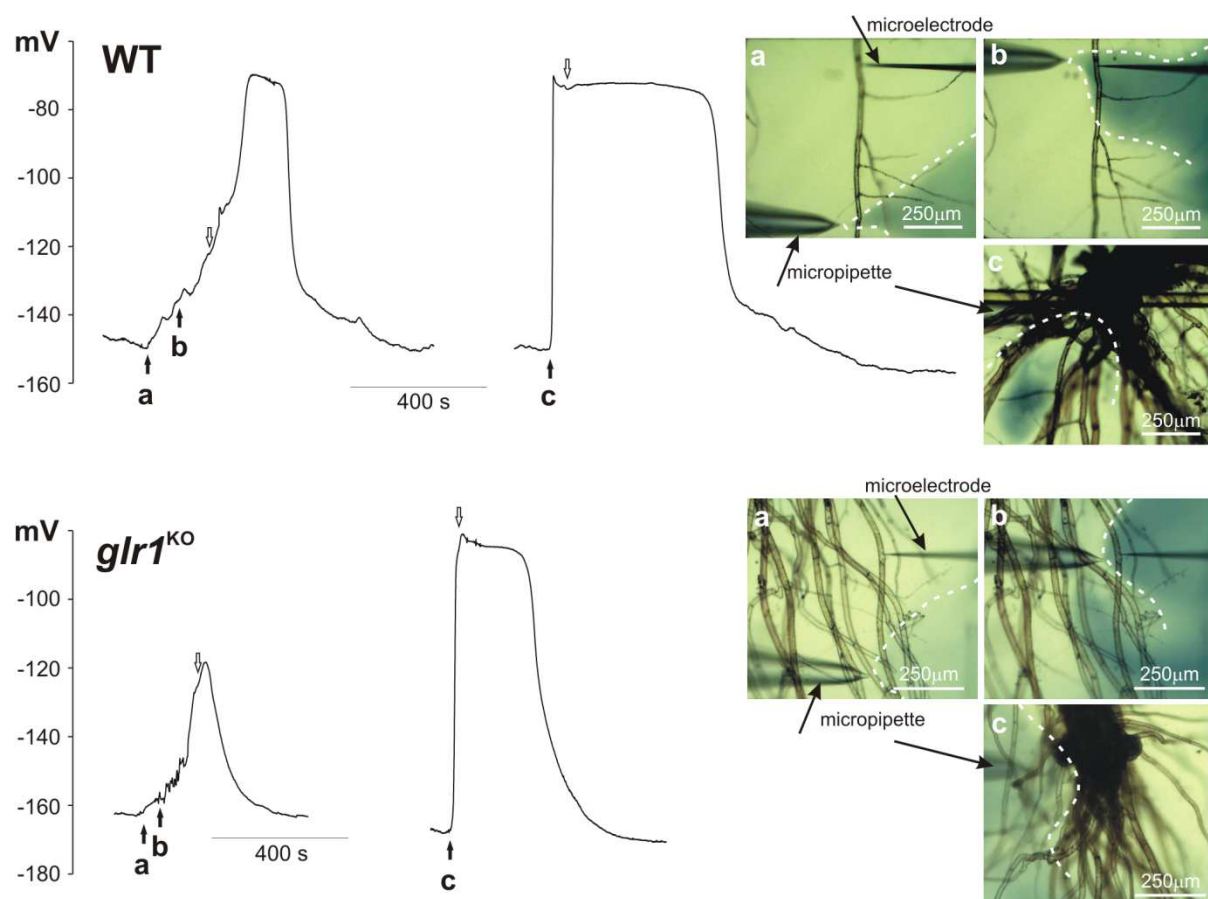


828 **Fig. 2.** Blockage of H₂O₂-evoked long-distance electrical signals by 2 mM lanthanum (A) and
829 0.5 mM EDTA (B). The method of stimulation was the same as in Fig. 1A. The representative
830 membrane potential changes show the effects of preincubation in lanthanum (A) or EDTA
831 (B), respectively, and then washout of the drugs carried out on the same plant.

832

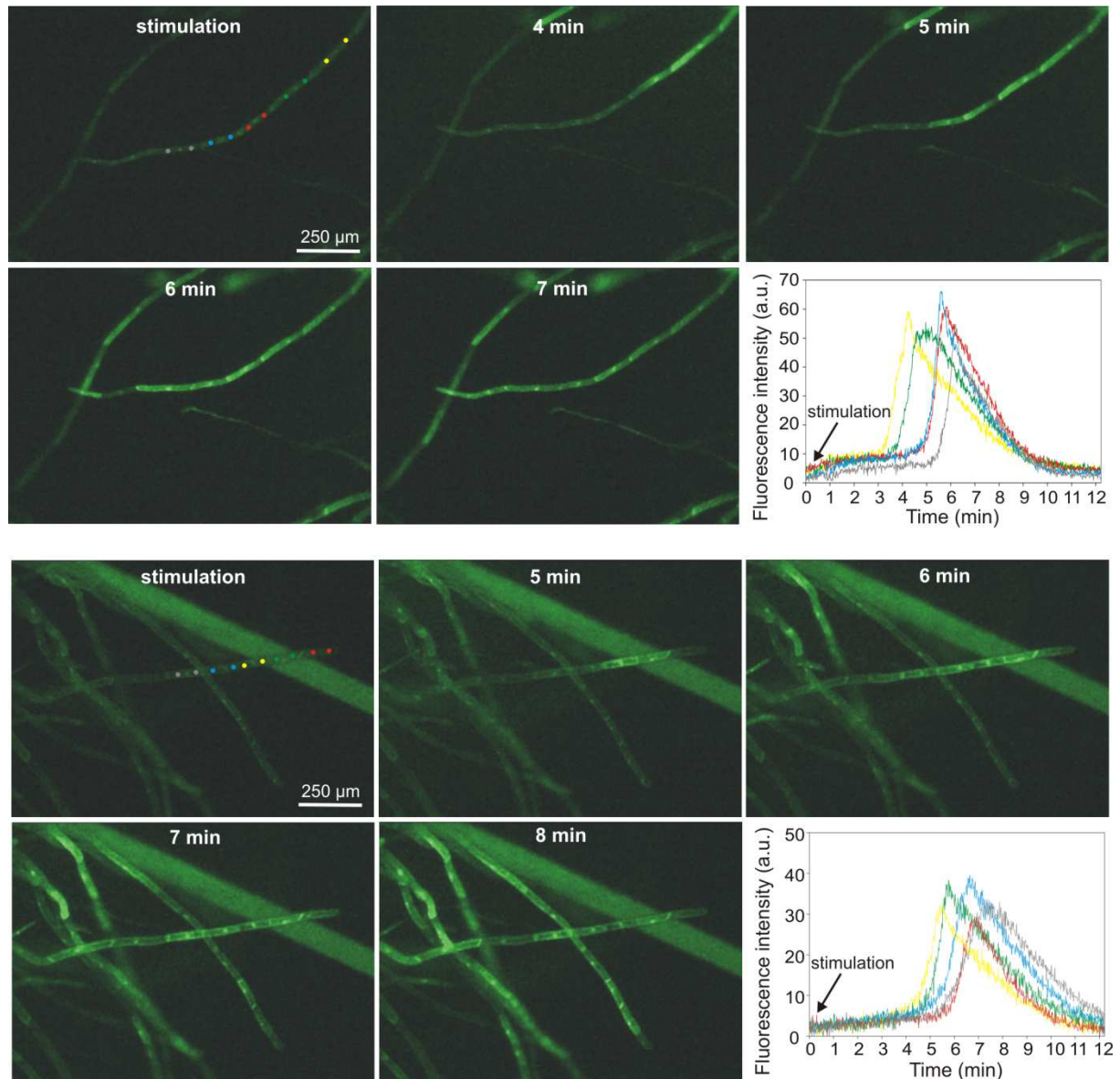


834 **Fig. 3.** Comparison of H₂O₂-evoked long-distance electrical signals recorded in wild type and
835 *Ppplr1*^{KO} mutant. The method of stimulation was the same as in Fig. 1A.

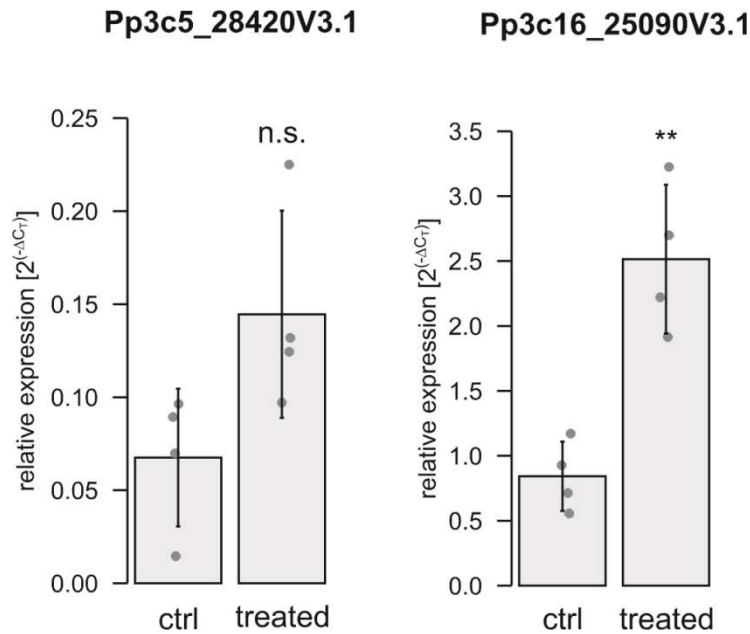


836

837 **Fig. 4.** Hydrogen peroxide-evoked membrane potential changes recorded in protonema cells
838 from wild type and *Pp**glr1*^{KO} mutant. Hydrogen peroxide (0.5 mM) was injected into the
839 selected site by the micropipette. In the pictures placed on the right side of presented traces,
840 three different measurement variants are presented: a - stimulation of the cells adjacent to the
841 tested cell (site of the microelectrode insertion), b - direct stimulation of the tested cell, and c
842 - stimulation of the basal part of the gametophyte. The pictures show dispersion of H₂O₂
843 stained with 1 mM aniline blue (marked by dashed white lines) recorded 5 seconds after time
844 points a, b, and c marked on the trace by black arrows. The end of stimulation (removal of the
845 micropipette from the measuring chamber) was marked by white arrows.



847 **Fig. 5.** Hydrogen peroxide-evoked calcium signals recorded in protonema cells expressing
848 fluorescent calcium biosensor GCaMP3. For each cell two circular ROIs (Region of Interest)
849 located in cytoplasmic region from both sides of the nucleus were analyzed. The two panels
850 of pictures show two different types of calcium signal propagation - at the upper the signal
851 propagate in one direction starting from the site of stimulation (basal part of the gametophyte)
852 and at lower panel, the signal propagation starts from one cell (marked by yellow ROIs) and
853 propagate in two opposite directions. Recorded during the experiment changes in fluorescence
854 intensity in different ROIs are presented in the bottom right corner of each picture panels.



855

856 **Fig. 6.** Gene expression analysis by qPCR of selected gene candidates. Apices were used
857 from untreated gametophores and gametophores treated at the base with 0.5 mM H₂O₂ for 8
858 min. Dots represent biological replicates (mean values from three technical replicates). Bars
859 are mean values from the four biological replicates with standard deviation. Relative
860 expression (2^(-ΔCT)) of Pp3c5_28420V3.1 and Pp3c16_25090V3.1 is calculated against the
861 reference genes L21 (Pp3c13_2360V3.1) and LWD (Pp3c22_18860V3.1) according to Livak
862 & Schmittgen (2001). Significance levels are based on a one-way Anova with subsequent
863 post-hoc test (**p < 0.01); n.s. = not significant.

864

865

866

867

868

869

870

871

872

873 **Table 1. Values of electrical signal parameters obtained in leaf cells after the application**
 874 **of hydrogen peroxide in different concentrations and different variants of experiments.**

	V_0 (mV)	V_{max} (mV)	A (mV)	$t_{1/2}$ (s)	R_{dep} (mV/s)
basal stimulation 0.5 mM	-154±3 (n=19)	-86±3 ^{a, b, c,} _{d, e} (n=19)	68±3 ^{a, b, c} (n=19)	236±44 ^a (n=17)	14.5±1.6 ^{a, b,} _{c, d, e} (n=18)
basal stimulation 0.1 mM	-161±4 (n=14)	-123±6 ^{d, i} (n=14)	38±6 ^g (n=14)	169±33 (n=13)	6±1.4 ^e (n=13)
basal stimulation 0.05 mM	-158±2 (n=12)	-121±7 ^{e, j} (n=12)	37±6 ^h (n=12)	140±15 (n=11)	4.4±1 ^d (n=11)
apical stimulation 0.5 mM	-165±5 (n=13)	-142±8 ^{a, f, k} (n=9)	22±5 ^{b, e, j} (n=9)	85±20 ^{c, f} (n=8)	2.3±0.4 ^b (n=8)
direct apical stimulation 0.5 mM	-153±4 (n=9)	-136±7 ^{b, g, l} (n=9)	17±7 ^{a, d, i} (n=9)	89±28 ^{d, g} (n=8)	2.9±1.6 ^a (n=6)
direct apical stimulation 5 mM	-153±5 (n=11)	-75±5 ^{f, g, h, i,} _j (n=11)	78±4 ^{d, e, f, g,} _h (n=11)	316±52 ^{e, f, g} (n=11)	11.6±3.5 (n=9)
basal stimulation of plant without rhizoids 0.5 mM	-156±3 (n=15)	-130±7 ^{c, h, m} (n=12)	24±5 ^{c, f, k} (n=12)	51±12 ^{a, b, e} (n=12)	3.3±0.8 ^c (n=12)
basal stimulation of plant without rhizoids 5 mM	-153±3 (n=10)	-86±6 ^{k, l, m} (n=10)	67±6 ^{i, j, k} (n=10)	389±79 ^{b, c, d} (n=9)	10.5±2.1 (n=10)

875 Table Footnote: Basal stimulation, apical stimulation, direct apical stimulation and basal
 876 stimulation of plant without rhizoids represent the variants of experiments presented in Fig.
 877 1A, B, C and D, respectively. The values denote mean ± standard error. Dunn's test was
 878 performed for all pairwise comparisons (P<0.05). V_0 - value of the membrane potential before
 879 stimulation, V_{max} - maximum value of the membrane potential recorded during the response,
 880 A - amplitude of the response, R_{dep} - the rate of depolarization measured in half of the
 881 amplitude on a section equal to the half of the amplitude, $t_{1/2}$ - duration of the response
 882 measured in half of the amplitude, n-number of tested plants.

883 **Table 2. Values of electrical signal parameters obtained in leaf cells after the application**
 884 **of 0.5 mM hydrogen peroxide in the basal part of the gametophyte.**

	V_0 (mV)	V_{max} (mV)	A (mV)	$t_{1/2}$ (s)	R_{dep} (mV/s)
standard (WT)	$-154 \pm 3^{a, b, c}$ (n=19)	$-86 \pm 3^{a, b, c}$ (n=19)	$68 \pm 3^{a, b, c, d}$ (n=19)	236 ± 44 (n=17)	$14.5 \pm 1.6^{a, b, c, d}$ (n=18)
2 mM La³⁺	-130 ± 3^b (n=19)	$-128 \pm 5^{a, d}$ (n=9)	$9 \pm 2^{a, e}$ (n=9)	205 ± 25 (n=3)	$0.5 \pm 0.2^{a, e}$ (n=8)
after washout of 2 mM La³⁺	-130 ± 4^c (n=19)	-104 ± 5 (n=5)	27 ± 4^d (n=4)	224 ± 34 (n=15)	3.6 ± 0.8^c (n=14)
0.5 mM EDTA	$-122 \pm 5^{a, d, e}$ (n=18)	-115 ± 7^c (n=9)	13 ± 4^b (n=9)	126 ± 32 (n=6)	$1.4 \pm 0.7^{b, f}$ (n=7)
after washout of 0.5 mM	-144 ± 4^e (n=18)	-121 ± 7^b (n=8)	24 ± 6^c (n=8)	63 ± 14 (n=7)	2.5 ± 0.7^d (n=7)
standard (Pp<i>glr1</i>^{KO})	-146 ± 3^d (n=26)	-100 ± 4^d (n=26)	46 ± 3^e (n=26)	194 ± 21 (n=25)	$9.6 \pm 1.2^{e, f}$ (n=24)

885 Table Footnote: The responses recorded in the wild type (WT) were obtained in the standard
 886 solution or the standard solution supplemented with 2 mM LaCl₃ or 0.5 mM EDTA. The *P.*
 887 *patens* knockout mutants (Pp*glr1*^{KO}) were tested in the standard solution. Explanations - as in
 888 Table 1.

889

890

891

892

893

894

895

896 **Table 3. Values of parameters of electrical signals in protonema cells after the**
 897 **application of 0.5 mM hydrogen peroxide directly/indirectly to the cell or in the basal**
 898 **part of the gametophyte.**

	V_0 (mV)	V_{max} (mV)	A (mV)	$t_{1/2}$ (s)	R_{dep} (mV/s)
direct/indirect stimulation (WT)	-155±8 (n=8)	-89±9 (n=8)	66±6 (n=8)	403±105 (n=7)	1.6±0.6 ^{a, d} (n=8)
basal stimulation (WT)	-155±7 ^{d, h} (n=8)	-74±4 (n=8)	81±4 ^a (n=8)	486±100 (n=8)	9.3±2.5 ^{a, b} (n=8)
direct/indirect stimulation (Pp<i>glr</i>^{KO})	-146±4 (n=10)	-84±5 (n=10)	63±4 ^a (n=10)	300±70 (n=10)	1.1±0.3 ^{b, c} (n=10)
basal stimulation (Pp<i>glr1</i>^{KO})	-155±2 (n=10)	-77±3 (n=10)	78±3 (n=10)	294±25 (n=9)	8.9±3 ^{c, d} (n=10)

899 Table Footnotes: Direct and indirect stimulation correspond to the measuring variants
 900 presented at Fig. 4. Explanations - as in Table 1.

901

902

903

904

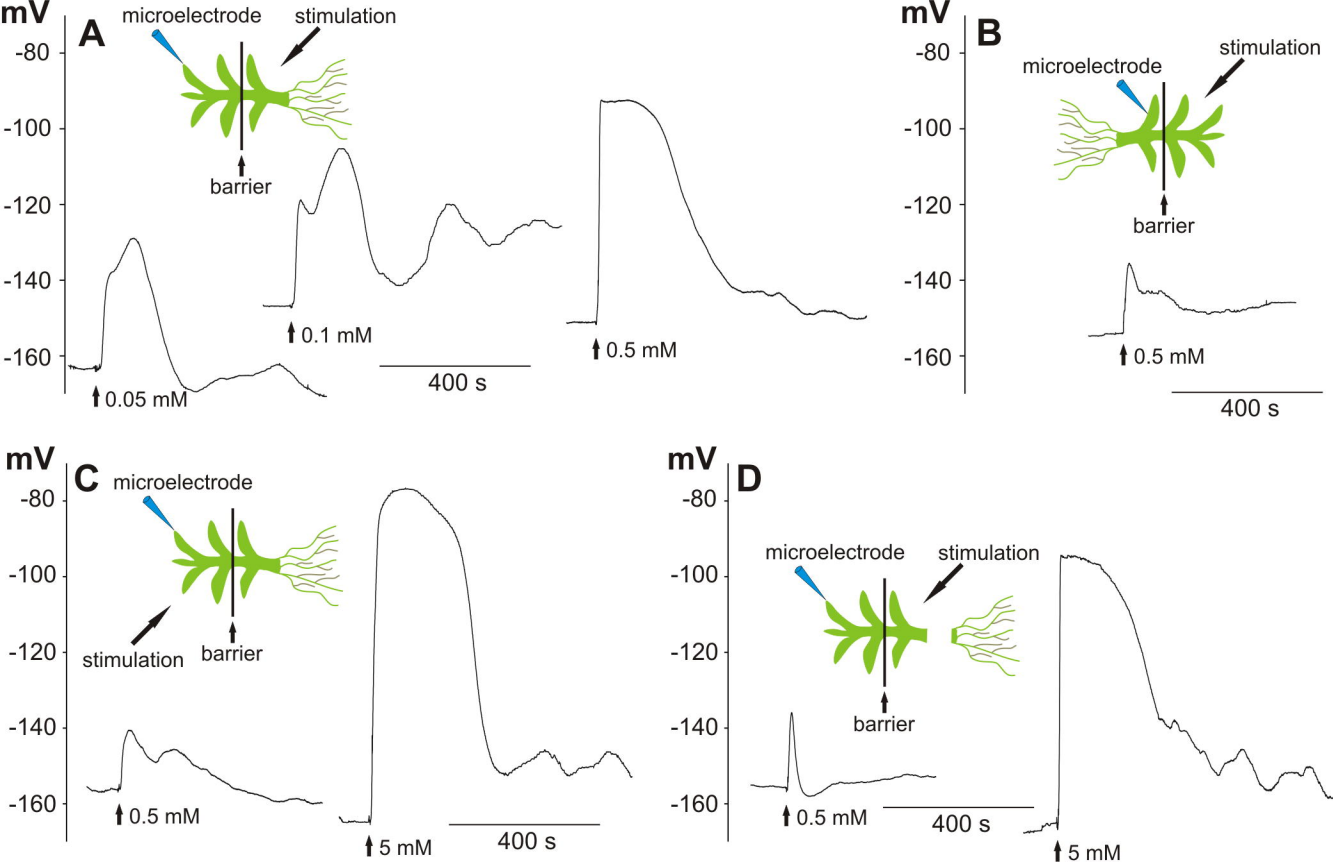
905

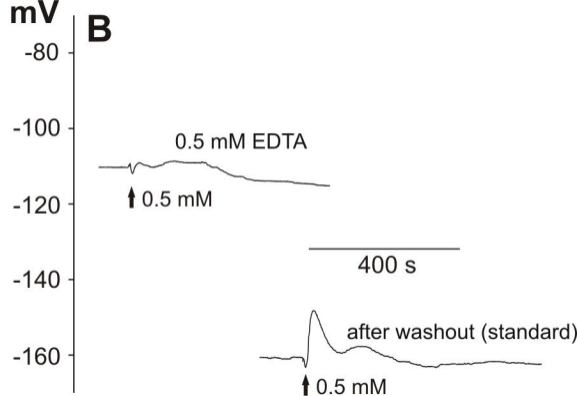
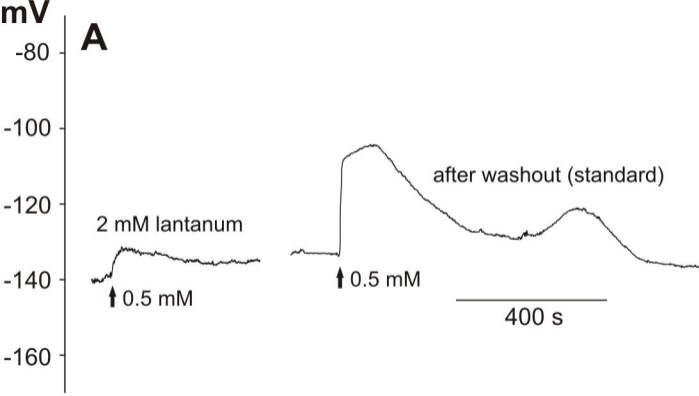
906

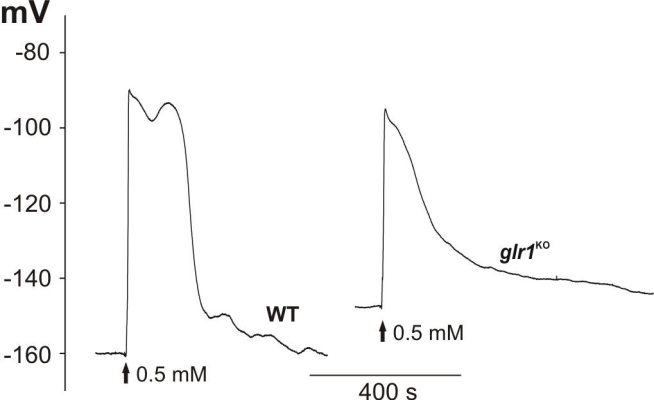
907

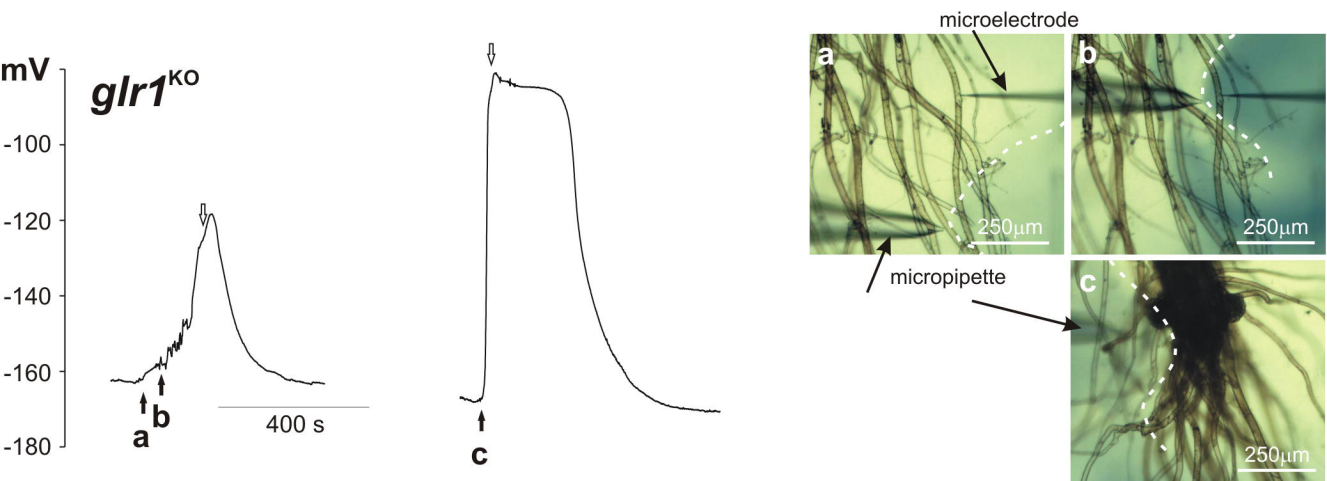
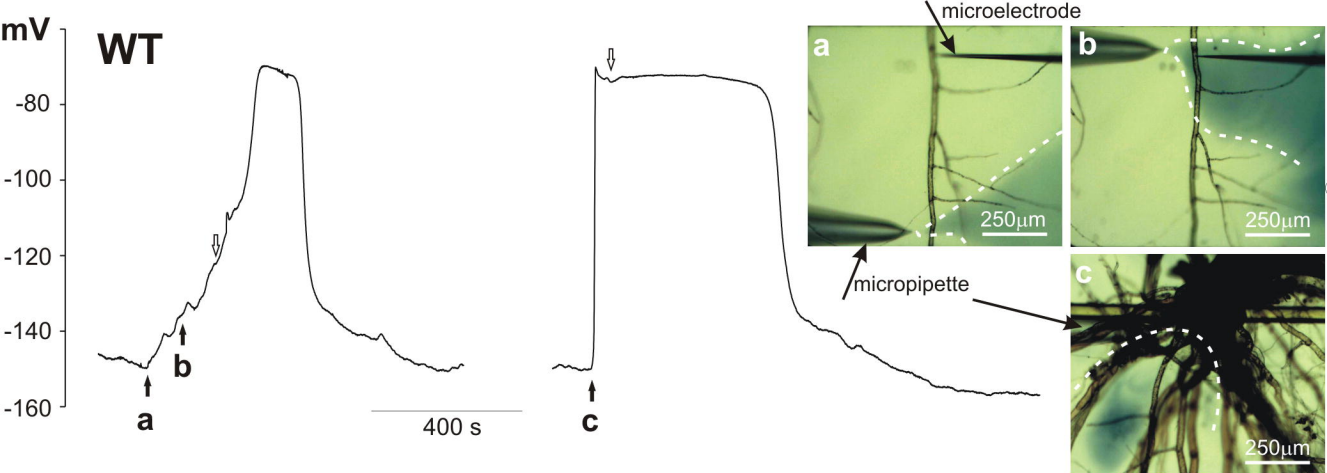
908

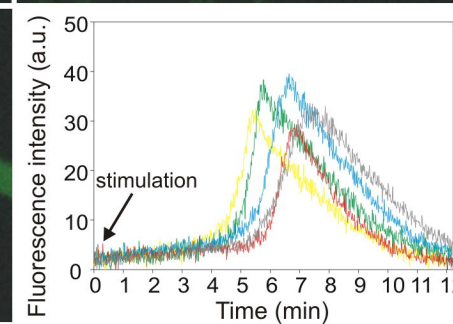
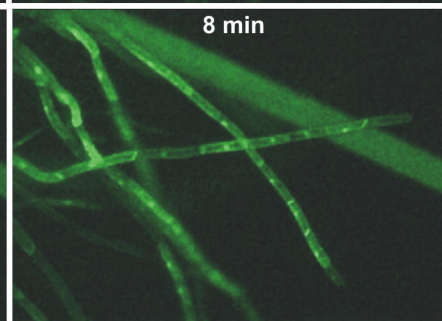
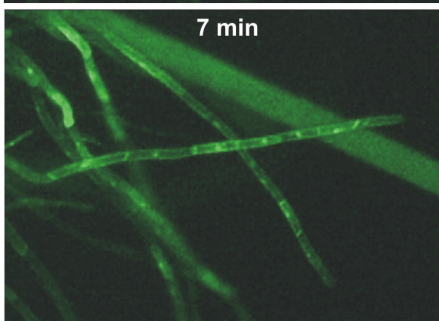
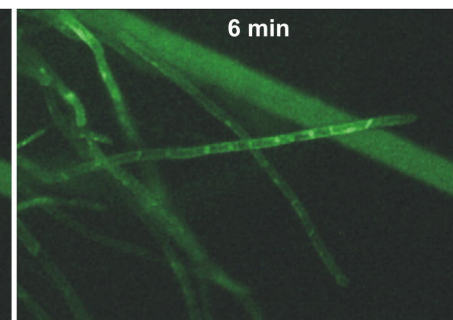
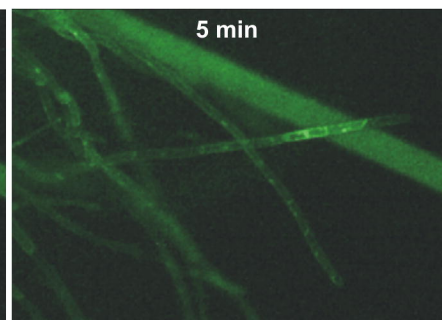
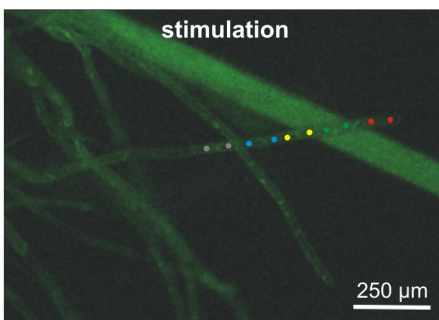
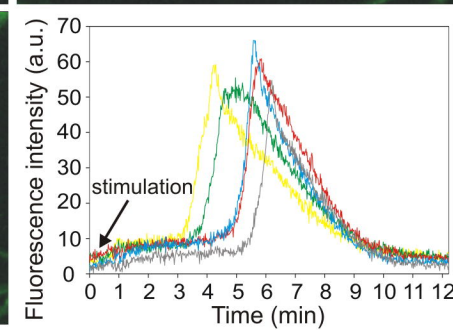
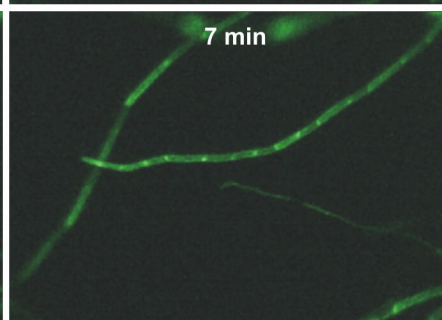
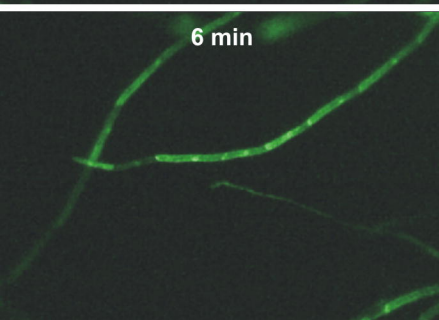
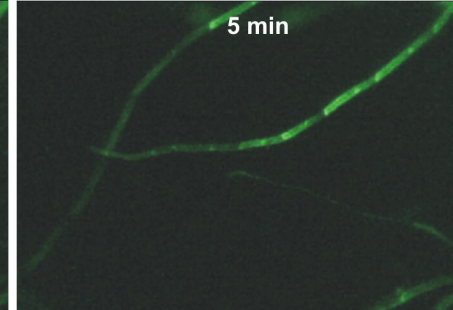
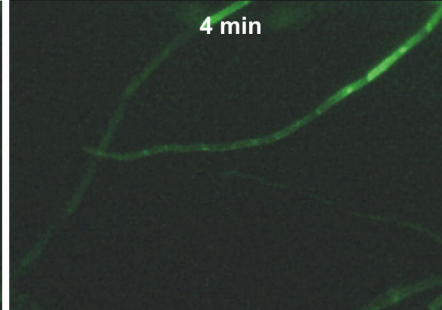
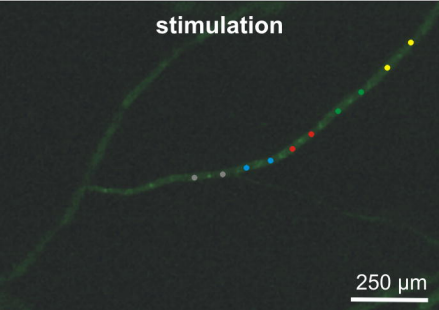
909



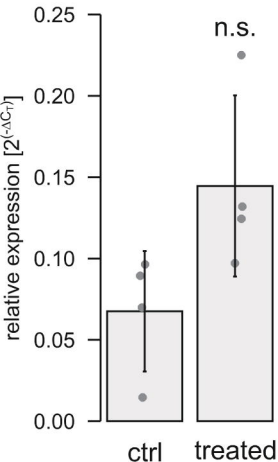








Pp3c5_28420V3.1



Pp3c16_25090V3.1

